

University of Louisville

ThinkIR: The University of Louisville's Institutional Repository

Electronic Theses and Dissertations

5-2015

Data driven comprehensive assessment of the performance of stormwater best management practices.

Shanshan Li
University of Louisville

Follow this and additional works at: <https://ir.library.louisville.edu/etd>



Part of the [Civil Engineering Commons](#)

Recommended Citation

Li, Shanshan, "Data driven comprehensive assessment of the performance of stormwater best management practices." (2015). *Electronic Theses and Dissertations*. Paper 2069.
<https://doi.org/10.18297/etd/2069>

This Doctoral Dissertation is brought to you for free and open access by ThinkIR: The University of Louisville's Institutional Repository. It has been accepted for inclusion in Electronic Theses and Dissertations by an authorized administrator of ThinkIR: The University of Louisville's Institutional Repository. This title appears here courtesy of the author, who has retained all other copyrights. For more information, please contact thinkir@louisville.edu.

DATA DRIVEN COMPREHENSIVE ASSESSMENT OF THE PERFORMANCE OF
STORMWATER BEST MANAGEMENT PRACTICES

By

Shanshan Li

B.E. in Environmental Engineering, Shandong University of Science and Technology, QingDao, China, 2007

M.E. in Environmental Engineering, North China Electric Power University, Beijing, China, 2011

A Dissertation

Submitted to the Faculty of the

J.B. Speed of Engineering of the University of Louisville

in Partial Fulfilment of the Requirements

for the Degree of

Doctor of Philosophy

in Civil Engineering

Department of Civil and Environmental Engineering

University of Louisville,

Louisville, Kentucky

May 2015

Copyright 2015 by Shanshan Li

All rights reserved

DATA DRIVEN COMPREHENSIVE ASSESSMENT OF THE PERFORMANCE OF
STORMWATER BEST MANAGEMENT PRACTICES

By

Shanshan Li

B.E. in Environmental Engineering, Shandong University of Science and Technology, QingDao, China, 2007

M.E. in Environmental Engineering, North China Electric Power University, Beijing, China, 2011

A Dissertation Approved on

April 3, 2015

By the following dissertation committee

Dr. Thomas D. Rockaway

Dr. J. P. Mohsen

Dr. Zhihui Sun

Dr. Olfa Nasraoui

DEDICATION

To my parents

ACKNOWLEDGEMENTS

As the overflow problem has become an issue for many cities, I'm glad I could work on a PhD thesis related to stormwater best management practices, and it is very interesting to advise the stakeholder about the performance of the stormwater best management practices.

I would like to offer my heartfelt thanks to all those who supported and assisted me during my PhD research. First and foremost, my utmost gratitude goes to my academic adviser Dr. Thomas D. Rockaway who inspired my research and broadened my horizon. Without his guidance, encouragement, and support, I would never have been able to finish my dissertation.

I also would like to express my thanks to my dissertation committee of Dr. J. P. Mohsen, Dr. Zhihui Sun, and Dr. Olfa Nasraoui for their support over the past two years as I move from an idea to a completed study. I want to give my thanks to Joshua Rivard and Hamidreza Kazemi who always efficiently provide support in data collection and advice in data validation. In addition, my genius friend Gopi Chand Nutakki offered a massive support on Java programming. I really appreciated it.

Specially, I would like to thank Dr. J. P. Mohsen and the Department of Civil and Environmental Engineering at the University of Louisville for the financial support. Also, I would like to thank all my course teachers during my PhD period, who helped to lay a solid foundation for my academic research.

ABSTRACT

DATA DRIVEN COMPREHENSIVE ASSESSMENT OF THE PERFORMANCE OF STORMWATER BEST MANAGEMENT PRACTICES

Shanshan Li

March 26th, 2015

In order to evaluate the performance of the stormwater best management practices (BMPs) installed on the Belknap campus at the University of Louisville, a comprehensive assessment on the stormwater BMPs' the flow volume reduction, peak flow attenuation, and overflow area abatement was made.

We used a two-pronged analysis based on 1) predictive modeling using data mining approach; 2) model-based hydraulic simulation. The novelty of study is that it not only assessed the stormwater BMPs' performances on flow volume reduction, but also assessed their performance on peak flow attenuation which is neglected in previous studies and assessment practices. Flow volume reduction and peak flow attenuation were assessed through mining the rainfall and combined sewer flow data before and after the BMPs' installation. The stormwater BMPs' performances on overflow area abatement were assessed through contrasting the overflow areas before and after the BMPs' installation.

The radar rainfall data was verified using the local rain gauge data, and the rainfall event is sorted out using a 6 hour dry period. The data mining in this study includes rainfall data validation, data preparation, and modelling. The predictive Multiple Linear Regression Models (MLRMs) and Back Propagation Neural Network Models (BPNNM) were built.

For the study area, flow volume in wet weather is mostly controlled by rainfall depth, and followed rainfall duration. Peak flow is decided by rainfall depth, peak rainfall intensity, duration and duration of above average rainfall intensity. Peak flow is negatively correlated with rainfall duration, while positively correlated with other three features.

According to both model, the estimated volume of the flow diverted by the stormwater BMPs are approximately 30 million gallons per year, and the magnitude of the peak flow could be trimmed down by approximately 50%. Multiple linear regression and back-propagation neural network are evaluation methods which are not only applicable in the studied case, but also can be widely adopted. However, it shows that the BPNNM is only viable to predict for flow volume lower than 6 million gallons.

The overflow area abatement was assessed through contrasting the overflow areas before and after the installation of the stormwater BMPs. Overflow areas were visualized by performing coupled 1D/2D hydraulic simulation.

It shows that the overflow areas, which could be saved by the stormwater BMPs, depend on the magnitude of the rainfall event. The abatement in overflow areas is more evident at

4 inch rainfall event and the 1 inch rainfall event. In the 4 inch rainfall event, the overflow areas at the JB Speed School parking lot, Student Rec Center, and College of Business were significantly abated by the stormwater BMPs.

TABLE OF CONTENTS

CHAPTER I.....	- 1 -
INTRODUCTION	- 1 -
1.1 Stormwater Best Management Practices	- 2 -
1.2 Purpose of This Study.....	- 4 -
1.3 Study Area	- 4 -
1.4 Methodology.....	- 7 -
1.5 Contributions.....	- 9 -
CHAPTER II.....	- 10 -
LITERATURE REVIEW	- 10 -
CHAPTER III	- 15 -
DATA SUMMARY	- 15 -
3.1 Data for Data Mining.....	- 15 -
3.1.1 Raw data.....	- 15 -
3.1.2 Data Preparation.....	- 17 -
3.2 Data for Hydraulic Simulation.....	- 29 -
CHAPTER IV	- 34 -
COMPREHENSIVE ASSESSMENT METHODOLOGIES	- 34 -
4.1 Flow Volume Reduction and Peak Flow Attenuation	- 34 -
4.1.1 Proposing Assumption for Modelling.....	- 35 -
4.1.2 Modelling Procedures	- 45 -

4.2 Overflow Area Abatement	- 69 -
4.2.1 Hydraulic Conditions	- 69 -
4.2.2 Simulation Scenarios	- 74 -
4.2.3 Simulation Job Control	- 79 -
CHAPTER V	- 81 -
RESULTS AND DISCUSSION	- 81 -
5.1 Flow Volume Reduction	- 81 -
5.2 Peak Flow Attenuation.....	- 86 -
5.3 Overflow Area Abatement	- 89 -
CHAPTER VI	- 93 -
CONCLUSIONS.....	- 93 -
6.1 Conclusions.....	- 93 -
6.2 Contributions.....	- 95 -
6.3 Future Work and Recommendations	- 96 -
6.4 Limitations	- 98 -
REFERENCES	- 99 -
APPENDIX.....	- 106 -
CURRICULUM VITAE.....	- 109 -

LIST OF TABLES

Table 1 Information of Stormwater BMPs Projects	- 6 -
Table 2 Two sample t-test for radar pixel 7492 and rain gauge TR12	- 20 -
Table 3 Two sample t-tests for radar pixel 7497 vs. rain gauge TR12 and radar pixel 8161 vs. rain gauge TR05	- 22 -
Table 4 Number of rainfall events pre- and post-installation of the stormwater BMPs-	27 -
Table 5 Denotation for direct rainfall features.....	- 44 -
Table 6 Descriptive Statistics of the Rainfall Features before Standardization.....	- 48 -
Table 7 Descriptive Statistics of the Rainfall Features after Standardization	- 48 -
Table 8 Important Rainfall Features Affecting Flow Volume and Peak Flow	- 50 -
Table 9 Fit-of-goodness for Flow Volume MLRM	- 53 -
Table 10 Analysis of Coefficients for Flow Volume MLRM	- 53 -
Table 11 Fit-of-goodness for Peak Flow MLRM	- 55 -
Table 12 Analysis of Coefficients for Peak Flow MLRM.....	- 56 -
Table 13 Flow Volume BPNNM Running Result	- 63 -
Table 14 Peak Flow BPNNM Running Result	- 65 -
Table 15 Status of the layers for the scenario 1.1	- 75 -
Table 16 Status of the layers for the scenario 1.2.....	- 76 -
Table 17 Status of the layers for the scenario 2.1	- 77 -
Table 18 Status of the layers for the scenario 2.2.....	- 78 -

LIST OF FIGURES

Figure 1. Location of study area and the areas installed stormwater BMPs..... - 8 -

Figure 2 Range of radar pixels and locations the rain gauges in Jefferson County..... - 18 -

Figure 3 Radar Pixel 7492 vs. Rain Gauges TR12 and TR05 - 19 -

Figure 4 Radar Pixel 7492 vs. Rain Gauges TR12 and TR05 - 21 -

Figure 5. Monthly rainfall Depth form radar pixel 7492, rain gauge TR12 and TR 05 during January 2009 and March 2014..... - 23 -

Figure 6. Monthly rainfall Depth form radar pixel 7497 and rain gauge TR12 during January 2009 and March 2014..... - 24 -

Figure 7 Monthly rainfall Depth form radar pixel 8161 and rain gauge TR05 during January 2009 and March 2014 - 25 -

Figure 8. The incremental rainfall depth and the cumulative depth of the rainfall event on 6/18/2011 - 27 -

Figure 9. Real-time rainfall intensity and flow rate before and after development of the stormwater BMPs..... - 28 -

Figure 10 Rainfall event occurred on June 18, 2011 - 30 -

Figure 11 Rainfall event occurred on May 29, 2012 - 30 -

Figure 12 Map of land use for the study area - 31 -

Figure 13 Ground elevation contours of the study area..... - 32 -

Figure 14 Combined sewer drainage system for the study area - 33 -

Figure 15. The probability distribution of dry period of the rainfall events - 37 -

Figure 16. The relationship of flow volume and rainfall depth before and after the installation of stormwater BMPs - 39 -

Figure 17. The relationship of flow volume and rainfall depth before and after the installation of stormwater BMPs	- 40 -
Figure 18. The relationship of flow volume and rainfall depth before and after the installation of stormwater BMPs	- 41 -
Figure 19. The relationship of peak flow and rainfall depth before and after the installation of stormwater BMPs	- 42 -
Figure 20. Real-time Rainfall-Runoff Rate for the event on June 18, 2011	- 44 -
Figure 21. Data mining flow chart.....	- 46 -
Figure 22. Result of rainfall feature selection for flow volume on Weka	- 50 -
Figure 23. Result of rainfall feature selection for peak flow on Weka.....	- 51 -
Figure 24. Normality test for the flow volume MLRM	- 54 -
Figure 25. Normality test for the peak flow MLRM	- 57 -
Figure 26. Correlation coefficients of the flow volume BPNNM with the change of learning rates, momentums, and hidden nodes	- 60 -
Figure 27. Correlation coefficients of the peak flow BPNNM with the change of learning rates, momentums, and hidden nodes	- 61 -
Figure 28. The structure of flow volume BPNN.....	- 64 -
Figure 29. The structure of peak flow BPNNM	- 66 -
Figure 30. Flow chart for flow volume reduction using stormwater BMPs' design parameters.....	- 68 -
Figure 31 Elements needed in the coupled 1D/2D hydraulic simulation	- 73 -
Figure 32 Hydraulics job control interface	- 79 -
Figure 33 2D job control interface.....	- 80 -

Figure 34 Actual and predicted flow volume for pre- and post-development of stormwater BMPs.....	- 82 -
Figure 35 Actual and reduced flow volume for the rainfall events after the development of stormwater BMPs.....	- 83 -
Figure 36 Total flow volume reduction by the stormwater BMPs	- 85 -
Figure 37 Actual and predicted flow volume for pre- and post-development of stormwater BMPs.....	- 87 -
Figure 38 Average peak flow attenuation by stormwater BMPs	- 88 -
Figure 39 Maximum Pre- and Post-BMPs Overflow Area caused by rainfall event on June 18, 2011.....	- 91 -
Figure 40 Maximum Pre- and Post-BMPs Overflow Area caused by rainfall event on May 29, 2012.....	- 92 -

CHAPTER I

INTRODUCTION

High intensity rainfall tends to create overland flow, especially on non-permeable concrete and asphalt ground. Enormous economic loss and tragic health damage could be caused by severe stormwater overland flow.

In this study, a data driven comprehensive assessment on the performance of the stormwater best management practices was made/implemented for the Belknap campus at the University of Louisville. The aspects of the assessment on the stormwater best management practices include flow volume reduction, peak flow attenuation, and overflow area abatement. As the construction of the stormwater best management practices may cost millions of dollars, the assessment will provide the effectiveness of the investment made by the stakeholders and useful guidance for the future decision makers.

The assessment results in this study might be only applicable to the situation on the Belknap campus at the University of Louisville, however, the performance assessments methods could widely be adopted, especially in similar situations.

1.1 Stormwater Best Management Practices

The urbanization of watersheds, with the associated increase in impervious surface and intensity of use, changes the local hydrology and that of the downstream river systems (Heasom, Traver et al. 2006). In an effort to reduce the impact of development, many communities are implementing “green infrastructure”. Green Infrastructure could be described as techniques, measures or structural controls used to manage the quantity and improve the quality of stormwater runoff using a network of natural and semi-natural areas, features and green spaces in the rural and urban areas (Naumann, Davis et al. 2011).

Stormwater Best Management Practices (BMPs) are the combination of permeable pavement, infiltration trench, infiltration basin, green roof, rain gardens, and rain barrels. commonly incorporated into the urban environment (Thorndahl and Rasmussen 2012, USEPA 2013). They are designed to divert stormwater from entering a communities combined sewer or the community’s waterways (URS 2012).

Theoretically, the installation of stormwater BMPs could recharge aquifer, increase the stormwater retention, improve water quality, reduce greenhouse gas emission, and reduce energy footprint. Studies have shown that stormwater BMPs are effective in runoff reduction (Rushton 2001, Hsieh and Davis 2005, Zachary Bean, Frederick Hunt et al. 2007, Passeport, Hunt et al. 2009), and pollutants removal (Rushton 2001, Hunt, Jarrett et al. 2006, Passeport, Hunt et al. 2009). And they are more cost-effective than conventional infrastructures, and could provide a higher social and ecological value to the community

(ENTRIX 2010, Jaffe, Zellner et al. 2010, De Sousa, Montalto et al. 2012, European Commission 2013). Stormwater BMPs are gaining popularity in the United States and around the world.

The cost of stormwater BMPs construction range from \$3,500 to \$125,000 depending on the type of BMPs, and the operation and management cost is usually 1% - 13% of the construction cost (Weiss, Gulliver et al. 2007). Many cities, such as Portland, Seattle, Philadelphia, Kansas City, New York, Washington D.C., Austin, San Diego, Louisville, Iowa City, Lynchburg, St. Louis, etc., have invested or are investing hundreds of millions of dollars on the installation of BMPs (Wise, Braden et al. 2010, CleanRiverCampaign 2014).

Therefore, the legit questions are: are the stormwater BMPs working as effectively as they were designed to? What is the volume of reduced stormwater? Are the stormwater BMPs able to attenuate the peak flow of the stormwater runoff? What is the degree of the attenuation? Have the stormwater BMPs helped abate the overflow area? To what extent?

Up until now, there has been very little work performed to prove performance of these BMPs systems. Most assessments are based on visual observations, basic data, or vague assessments, there is not a quantifiable methodology to determine if the systems are providing the intended results. Therefore, a comprehensive performance assessment on the BMPs is necessary.

1.2 Purpose of This Study

In view of the lack of effective techniques on the performance assessment of the costly stormwater BMPs, the purpose of this study is to develop methodologies that can assess overall performances on in-place stormwater BMPs utilizing flow instrumentation data commonly employed by waste water utilities.

The assessments should be performed on three aspects: flow volume reduction, peak flow attenuation, and overflow area abatement. The quantitative magnitude of flow volume reduction, and peak flow attenuation, and a visual contrast of overflow area abatement should be obtained. The robustness of this system is that it does not rely on specialized instrumentation, rather utilizes flow monitoring data commonly recorded by waste water utilities.

1.3 Study Area

Combined sewer overflow caused by large storm events has been a very serious problem for the Belknap campus. While flooding during typically large rain events is common, the massive storm on August 4th, 2009 caused over \$20.9 million in flood damage. Apart from the enormous economic cost, the massive overflow leads to dangerous release of untreated sewage into the Ohio River, cause a threat to the residents' health and ecological integrity.

To remediate the flooding, a variety of Stormwater BMPs were designed and installed across the Belknap campus between 2011-2013, to more effectively manage stormwater and mitigate floods. According the University of Louisville, the BMPs were designed to capture over 127,000 ft³ of stormwater at a total cost of \$1.25 million.

Unfortunately, almost no instrumentation was included to verify that the installed stormwater BMPs are functioning as intended. The only instrumentation available is the flow meter FM0048 located on the cross section of West Cardinal Boulevard and South Forth Street. Figure 1 is the location of the study area, flow meter, and the location of the Stormwater BMPs. The information of stormwater BMPs projects developed on study area is listed in Table 1.

Table 1

Information of Stormwater BMPs Projects

Project ID	Name	Watershed Area (Square Feet)	Impervious Area (Square Feet)	Storage Capacity (Cubic Feet)
GP1	Grawemeyer South Parking Lot	139731	80209	16678
GO1	Grawemeyer Oval	173952	69349	34474
EL1	Esktrom Library	191560	108240	7500
EL2	Jouett Hall Rain Garden	34306	14397	7017
EL3	Law School Courtyard	18800	14240	7446
EL4	Law School Parking Lot	22612	19896	2485
BS1	Business School Parking Lot	95330	86052	8110
BS2	Music Building Roof/Cistern	41087	41087	10816
SM1	Speed Museum Base/Expand Infiltration	288624	213187	43868

(From Planning, Design, and Construction at University of Louisville)

1.4 Methodology

The limited amount of available instrumentation makes the assessment of the BMPs installed on the Belknap Campus challenging. Without data to gauge the performance of specific BMPs, a portfolio or watershed analysis approach was utilized to compare flow rates pre and post construction.

Data mining methods (such as multiple linear regression, artificial neural network) were conducted to correlate flow volume or flow rate with respective rainfall features. For the first time, detected rainfall and sewer flow data was utilized to assess the stormwater BMPs' performance on flow reduction and peak flow attenuation. Changes in the correlation values, and contrast on overflow areas can provide an indication of the relative effectiveness of the installed BMPs.

Also, a coupled 1D/2D hydraulic simulation was performed. Two rainfall events was investigated. The innovation of the assessment is that, in any given rainfall event, overflow areas on the two scenarios (Pre and Post-BMPs) was contrasted. There are four scenarios in total. The overflow area difference can indicate the effectiveness of the stormwater BMPs.

The conclusions in this study was focused on the University of Louisville's Belknap campus, however, the assessment methodologies are important, because it can be adaptable to other communities.

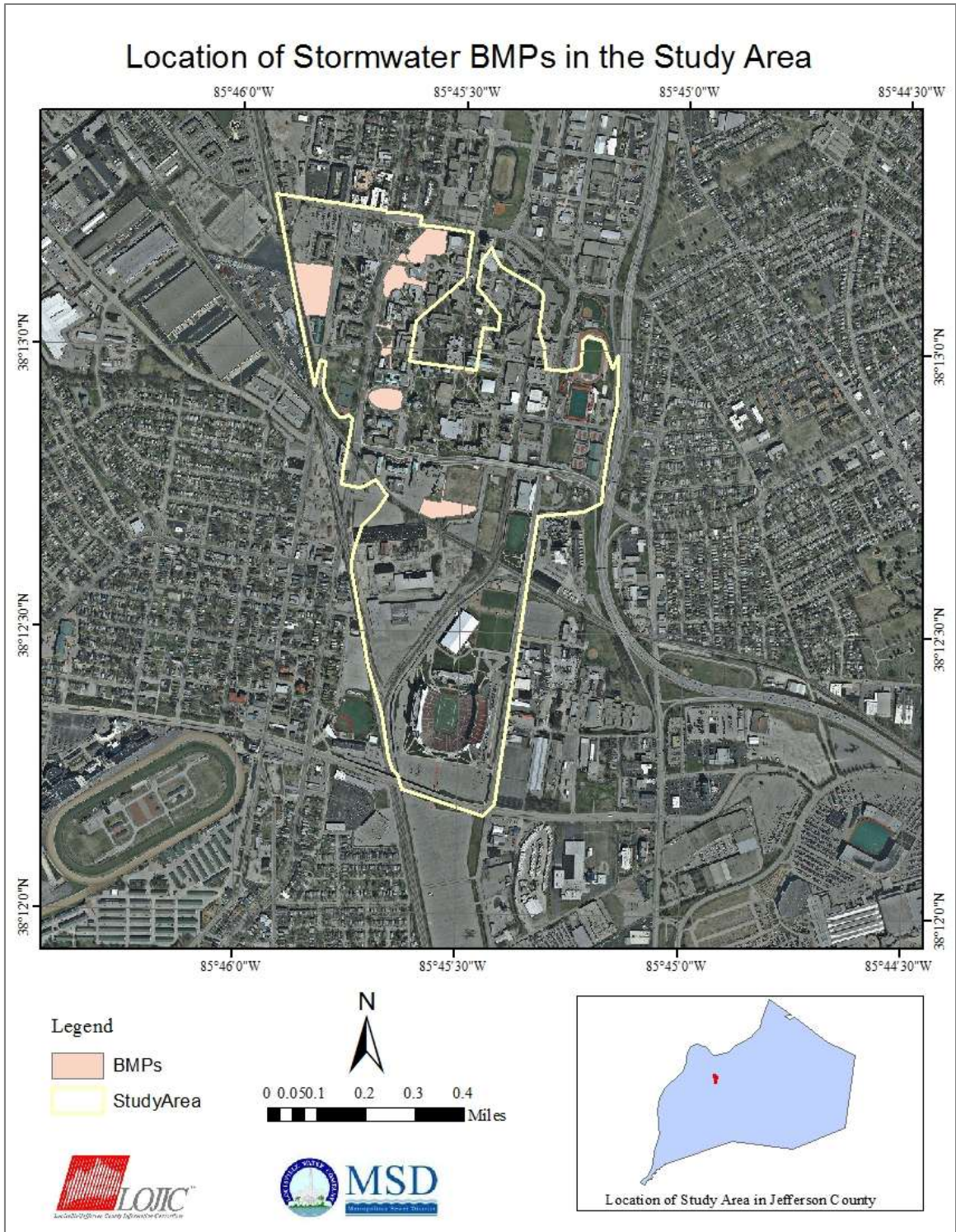


Figure 1. Location of study area and the areas installed stormwater BMPs

1.5 Contributions

The contributions of this study are listed as follows:

(1) It incorporated peak flow reduction as stormwater BMPs' performance assessment. The of rainfall – runoff assumption raised in this study linked rainfall features with flow volume/peak flow, which brought a new insight in solving stormwater BMPs' assessment problems. The assumption could be revised and adopted in many other situations.

(2) The volume of flow diverted by the stormwater BMPs for every rainfall/storm event in our study period was estimated, and the degree of peak flow attenuated was also predicted by the developed models.

(3) Multiple linear regression and back propagation neural network are feasible method in revealing the relationships either between flow volume and rainfall features, or between peak flow and rainfall features. The prediction accuracy and application range were also discussed.

(4) The overflow course was visualized in a coupled 1D/2D hydraulic simulation, and the overflow sensitive area could provide information needed for stakeholders and decision makers on the stormwater BMPs' installation priority.

CHAPTER II

LITERATURE REVIEW

During rain events, runoff from impervious surfaces, also known as urban runoff, is one of the leading causes of inundation damage and water quality impairment throughout the world (Strassler, Pritts et al. 2006). Flow control involves managing both the volume and intensity of stormwater discharge to receiving waters. High flow rates of stormwater discharge can cause a number of impacts and may also increase the pollutant concentration in stormwater runoff (Blink, Kelly et al. 2004).

Stormwater BMPs are control measures implemented to mitigate changes to both water quantity and quality of urban runoff (Reese and Debo 2002). They are used widely as a means for controlling flood runoff events, which have been proposed as an alternative approach to better mimic the natural flow regime by using decentralized design to control stormwater runoff at the source, rather than at a centralized location in the watershed (Damodaram, Giacomoni et al. 2010). Typically, stormwater BMPs can abate the overflow area during storm events through reducing the volume of the runoff by redirecting stormwater flow into the groundwater system. Simultaneously, it improves receiving water quality by attenuating peak flows of the runoff (Granato 2014).

The functions of the stormwater BMPs include reducing flow volume, attenuating peak flow, and abating overflow area. Therefore, a good performance of those functions are essential indicators for successful stormwater BMPs.

Runoff reduction (flow volume reduction) is the most frequently studied aspect of stormwater BMPs' performance. A variety of runoff reduction assessment tools have been developed, each with their own strengths and weaknesses.

The National Green Value Calculator (GVC) is a tool for quickly estimating runoff reduction (Technology 2006). When lot information, predevelopment condition, runoff reduction goal, conventional development, etc., are set, GVC could provide its estimation on the stormwater BMPs' runoff reduction performance momentarily. The pros of this tool are easy and fast, while the cons are the less accuracy and no peak flow assessment.

Similar to the National GVC, EPA's National Stormwater Calculator (SWC) is a desktop application that estimates the annual amount of rainwater and frequency of runoff from a specific site anywhere in the United States (including Puerto Rico), and the estimation is based on local soil conditions, land cover, and historical rainfall record (Infrastructure and Infrastructure 2013). Its pros and cons are the same with the National GVC.

Virginia Runoff Reduction Method (VRRM) is a relatively simple method to estimate the runoff volume reduction by using a designed excel file, which can be downloaded from the internet (Hirschman, Collins et al. 2008, Battiatia, Collins et al. 2010). It estimates the

volume of runoff reduction by the stormwater BMPs through the change of the land use, soil type, and hydraulic conditions before and after the installation.

There are also some assessment tools designed for special occasions. With regard to the overflow problem in urban areas, the U. S. Environmental Protection Agency (EPA) designed a Green LTCP-EZ Template as a tool to help small combined sewer overflow (CSO) communities develop their long-term overflow control plan (USEPA 2011). This model enables stakeholders to access the runoff volume reduction and CSO volume by importing the event precipitation, ground information and stormwater BMPs parameters.

In order to address the costs associated with vegetative roofs, rainwater catchment systems, and bioretention facilities, U.S. EPA developed Water Environment Research Foundation (WERF) BMP and LID whole life cost models. These tools can provide a framework to facility cost estimation for capital cost, operation and maintenance cost, and life-cycle net present value (Houdeshel, Pomeroy et al. 2010).

All these models mentioned above could be applied in assessing the performance of the chosen stormwater BMPs on the function of runoff reduction, and inform the stakeholder on decision making. However, as is known, high peak flow could cause serious damages in a flooding event, and is an indispensable part of flood control and management. Unfortunately, these models are all concerned with runoff volume reduction, none of them are capable of assessing the performance of stormwater BMPs on peak flows attenuation. Moreover, the value of runoff reduction provided by these models are calculated based on

surface water hydrology theory. None of them could provide a flow volume reduction at sewage level. As well, none of them could assess the flow volume reduction or peak flow attenuation utilizing the real-time monitored rainfall and sewer flow data.

For assessing the stormwater BMPs from a hydraulic perspective, the EPA Stormwater Management Model (SWMM) with LID Controls is one of the software packages most extensively used. It is a dynamic rainfall - surface runoff - subsurface runoff simulation model used for single-event to long-term simulation of the surface/subsurface hydrology quantity and quality (Rossman). It enables users to retrieve runoff volume and runoff rate by entering the meteorological data and land use characteristics (USEPA 2013). However, SWMM5, as with many other software platforms such as Storm NET, is hardwired to solve 4-6 iterations in the dynamic solution and proceeds to the next time step regardless of the correctness of the solution at that interval. This can generate continuity errors and also the wrong solution of the HGL. In SWMM5, the stored water is only in a constant area vs. depth shape.

As a stormwater management tool, coupled 1D/2D models are more accurate and produce results that are far more readily accepted and understood by managers, decision makers, and other stakeholders (Solutions 2004, Leandro, Chen et al. 2009). Unfortunately, the SWMM5 is not capable of offering 2D modeling as needed in a comprehensive performance assessment.

When comparing capabilities with the analysis engine of XPSWMM and programs such as SWMM5, the main consideration is the fact that XPSWMM is a fully dynamic model utilizing the St. Venant equations, which takes into account the hydraulic effects within a system occurring throughout a simulation which many other modeling platforms fail to estimate (Ovbiebo and She 1995, Othman Jaafar, Toriman et al. 2010).

Also, XPSWMM allows the water above the ground level (spillcrest) to be in a unique ponding shape at every node (Schaefer 2009). This ponding shape describes the sag that stores the water at a flooded manhole for example. This ponded volume can then be used to define required storage. Multi-links provide a tool which can model up to 7 items in parallel which share the same upstream and downstream nodes. This is a very convenient method to model numerous objects without drawing additional links.

These work exceptionally well for dual drainage scenarios (conduit flow and overland, street flow) or conduit flow with weir or bypass flows and can also be used to model bridge crossings in a 1D environment. Much more discussion can be provided on these topics as well as the 2D or coupled 1D/2D modeling capabilities offered by XPSWMM (Phillips, Yu et al. 2005, Toriman, Hassan et al. 2009).

CHAPTER III

DATA SUMMARY

The entire data utilized in this study includes the data for data mining and the data for hydraulic simulation. The assessment on flow volume reduction and peak flow attenuation were realized through data mining, which was about to conduct correlation between the monitored rainfall data and flow data. A series of rainfall data and flow data preparation should be performed before the actual modelling begins. Overflow area abatement was assessed through hydraulic simulation using XPSWMM software. The data needed is GIS files on elevation, land use, manhole information, sewer system information, etc.

3.1 Data for Data Mining

3.1.1 Raw data

In this study, the raw data applicable for this stormwater BMPs' assessments was comprised of rainfall data and sewer flow data pre and post the installation of stormwater BMPs.

The date range of the data is June 2011 — June 2013. All the data was collected, maintained, and provided by Louisville and Jefferson County Metropolitan Sewer District (MSD).

3.1.1.1 Rainfall Data

Application of weather radar data in urban hydrology is evolving, and it is applied in many scientific research areas (Pedersen, Jensen et al. 2010, Thorndahl and Rasmussen 2012). The study area is mainly covered by the three radar pixels (7492, 7493, and 7359). All the radar pixels are a 1000 meter \times 1000 meter in size. The real-time radar rainfall data would be calibrated by the rain gauges (TR05 and TR12) operated and maintained by Louisville MSD. Both the radar and the radar gauges were configured to record precipitation depth in inches detected during the previous 5 minutes period.

Additionally, a study accomplished by OneRain Inc., (Orangevale, CA) shows the NEXRAIN radar rainfall data system has performed very well since it was installed in MSD in October 2002 (Liu, Hoblit et al.).

3.1.1.2 Combined Sewer Flow Data

The real-time combined sewer flow data is measured by flow meters set up by Louisville MSD. The flow meters measure the flow rate in million gallons per day in 15 minutes intervals. The study area is part of the combined sewer watershed for flow meter FM0948.

The real-time combined sewer flow data provided by Louisville MSD enable us to extract peak flow and the total flow volume for each rainfall event.

3.1.2 Data Preparation

Data preparation is a crucial step in data mining. In this study, data preparation includes rainfall data validation and rainfall events preparation.

3.1.2.1 Rainfall Data Validation

In order to obtain valid quantitative precipitation estimates (Thorndahl and Rasmussen 2012), the local rain gauge data, which is also maintained by Louisville MSD, is used to calibrate the radar data (Steiner, Smith et al. 1999). Figure 2 is a map showing the radar pixels and rain gauges, and the distribution of the rain gauge stations in Jefferson County. The red area is the location of the study area, the pink drops are the locations of rain gauges utilized in this study, and the highlighted squares in green are the range of radar data.

The dilemma is there is no rain gauge placed in the study area. It is shown in the map, the nearest rain gauges to the study area are Nightingale Pump Station with an ID of TR12, Beargrass Creek Pump Station with an ID of TR05. TR12 and TR05 are located 2.5 miles and 4 miles away from the study area, and covered by the radar pixels 7497 and 8161 respectively.

Ranges of Radar Pixels and Locations of Rain Gauges

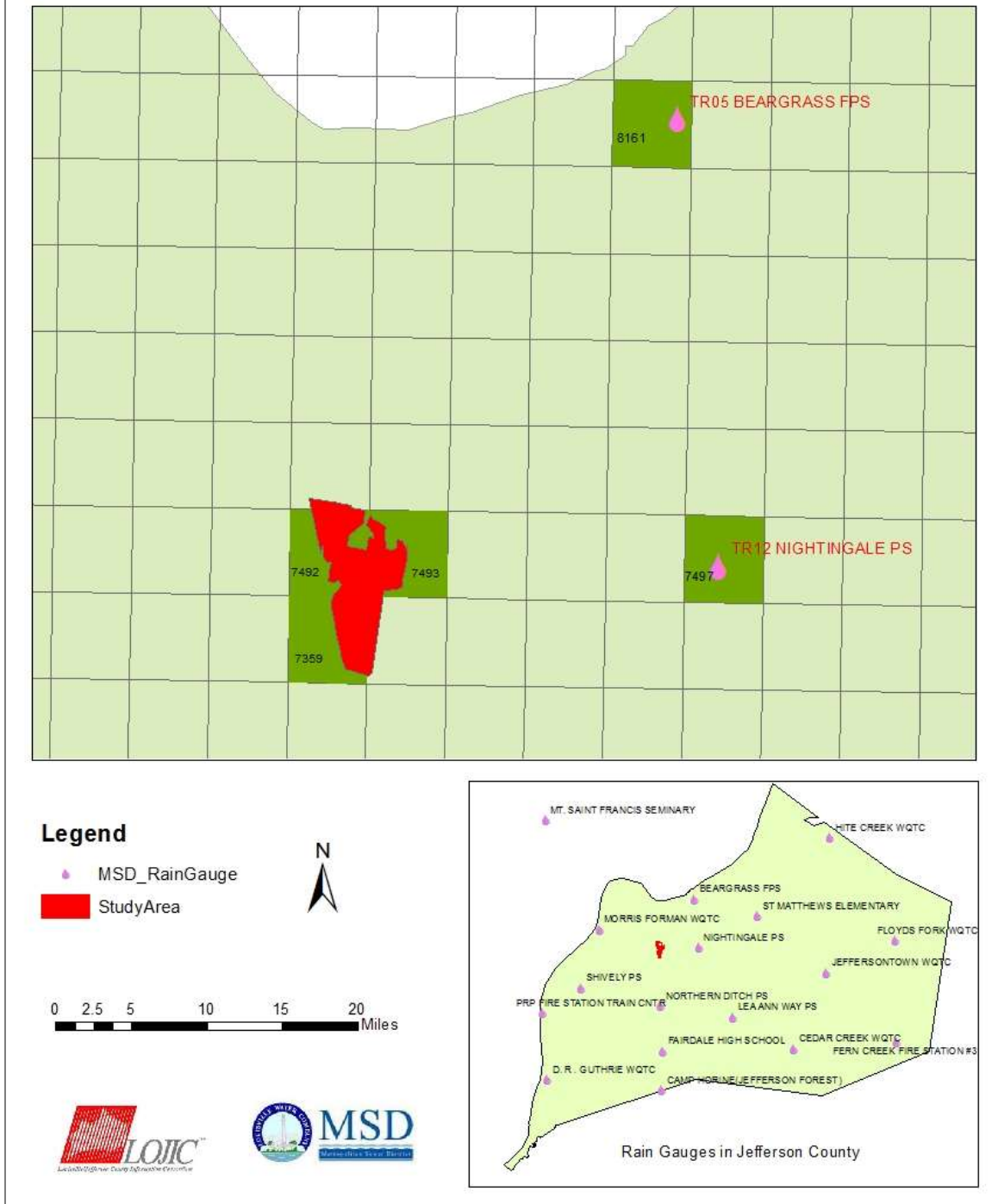


Figure 2 Range of radar pixels and locations the rain gauges in Jefferson County

Radar Pixel 7492 vs. Rain Gauges TR12 and TR05

As is shown in Figure 3, the radar pixel 7492 is one of the pixels that covers the study area. To investigate its reliability from January 2009 to March 2014, a comparison of monthly cumulative precipitation depth from radar pixel 7492 and its nearest rain gauges TR12 and TR05 was made (Figure 5). Two-sample t-tests on radar pixel 7492 vs. TR12 and radar pixel 7492 vs. TR05 were performed (Table 2), and the P-Values (probability of significance) are 0.009 and 0.002 (< 0.05), indicating the precipitation data from radar pixel 7492 is significantly different with that from rain gauge TR12 or TR05. The significant difference between radar pixel 7492 and its nearest rain gauges doesn't necessarily indicate the precipitation data from any of the sources are invalid. Rather, variation is expected as the rain gauges are located more than 2.4 miles away from the radar pixel 7492.

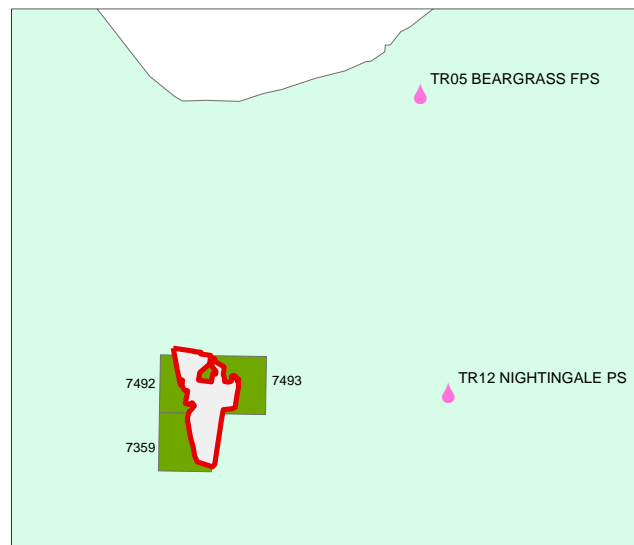


Figure 3 Radar Pixel 7492 vs. Rain Gauges TR12 and TR05

Table 2

Two sample t-test for radar pixel 7492 and rain gauge TR12

	Number of Samples	Mean	Standard Deviation	Mean Squared Error
Radar Pixel 9497	63	5.54	3.01	0.38
Rain Gauge TR12	63	4.22	2.54	0.32
Rain Gauge TR05	63	3.97	2.67	0.34

Difference = μ (Radar Pixel 9492) - μ (Rain Gauge TR12)

Estimate for difference: 1.321

95% CI for difference: (0.338, 2.305)

T-Test of difference = 0 (vs \neq): T-Value = 2.66 P-Value = 0.009 DF = 120

Difference = μ (Radar Pixel 9492) - μ (Rain Gauge TR05)

Estimate for difference: 1.574

95% CI for difference: (0.570, 2.578)

T-Test of difference = 0 (vs \neq): T-Value = 3.10 P-Value = 0.002 DF = 122

From Figure 2, it could be seen that rain gauge TR12 and TR05 fall in the perimeters of radar pixel 7497 and radar pixel 8181. Figure 6 and Figure 7 are the bar charts showing the monthly precipitation comparison for the two sources. Thus, if we could show the precipitation data from TR12 is similar to that from radar pixel 7497, and the precipitation data from TR05 is similar to that from radar pixel 8161 (Figure 4), it could be concluded that the rainfall radar data is reliable.

Two-paired t-tests were performed, and the results are shown in Table 3. The P-Value in the t-test is 0.754, and 0.848 respectively ($\gg 0.05$), which means the monthly precipitation data from radar pixel 7497 and rain gauge TR12 have no significant differences, and the monthly precipitation data from radar pixel 8161 and rain gauge TR05 have no significant differences. The high similarity of the rainfall data from different sources indicates the radar pixel precipitation data likely reflects the real precipitation level for the area it covers.

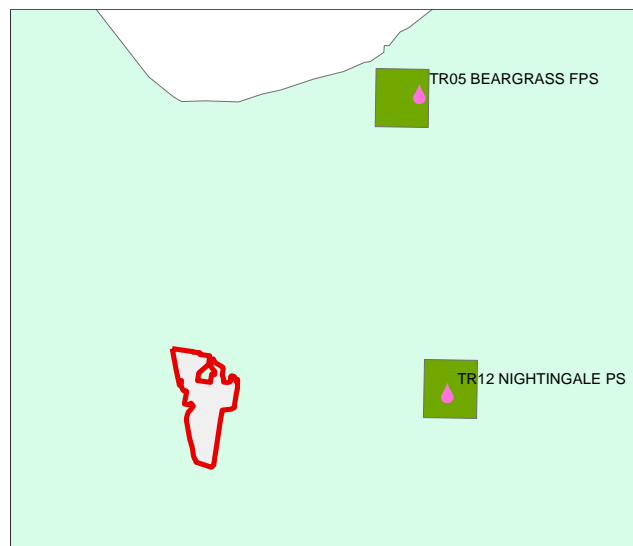


Figure 4 Radar Pixel 7492 vs. Rain Gauges TR12 and TR05

Table 3

Two sample t-tests for radar pixel 7497 vs. rain gauge TR12 and radar pixel 8161 vs. rain gauge TR05

	Number of Samples	Mean	Standard Deviation	Mean Squared Error
Rain Gauge TR12	63	4.22	2.54	0.32
Radar Pixel 9497	63	4.37	2.74	0.34
Rain Gauge TR05	63	3.97	2.67	0.34
Radar Pixel 8161	63	4.05	2.52	0.32

Difference = μ (Radar Pixel 9497) - μ (Rain Gauge TR12)

Estimate for difference: 0.148

95% CI for difference: (-0.783, 1.079)

T-Test of difference = 0 (vs \neq): T-Value = 0.31 P-Value = 0.754 DF = 123

Difference = μ (Radar Pixel 8161) - μ (Rain Gauge TR05)

Estimate for difference: 0.089

95% CI for difference: (-0.826, 1.004)

T-Test of difference = 0 (vs \neq): T-Value = 0.19 P-Value = 0.848 DF = 123

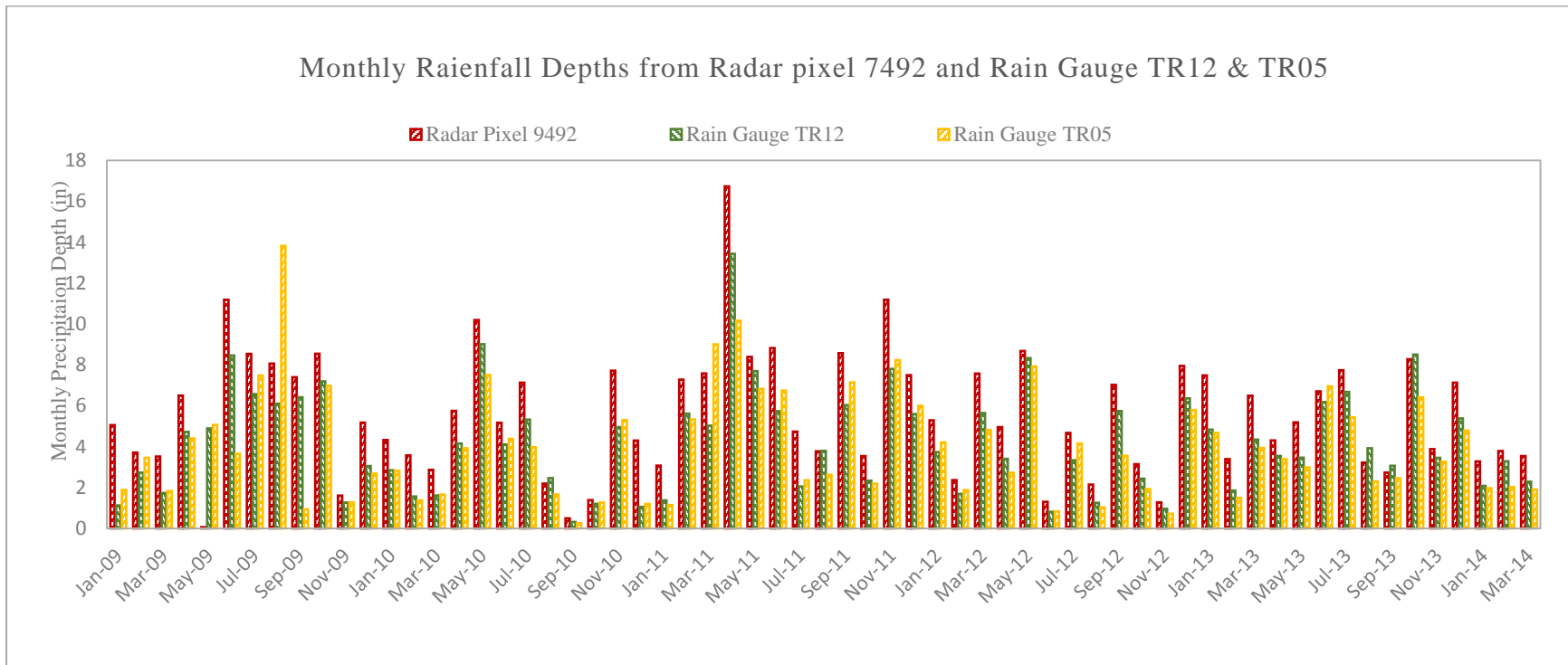


Figure 5. Monthly rainfall Depth form radar pixel 7492, rain gauge TR12 and TR 05 during January 2009 and March 2014

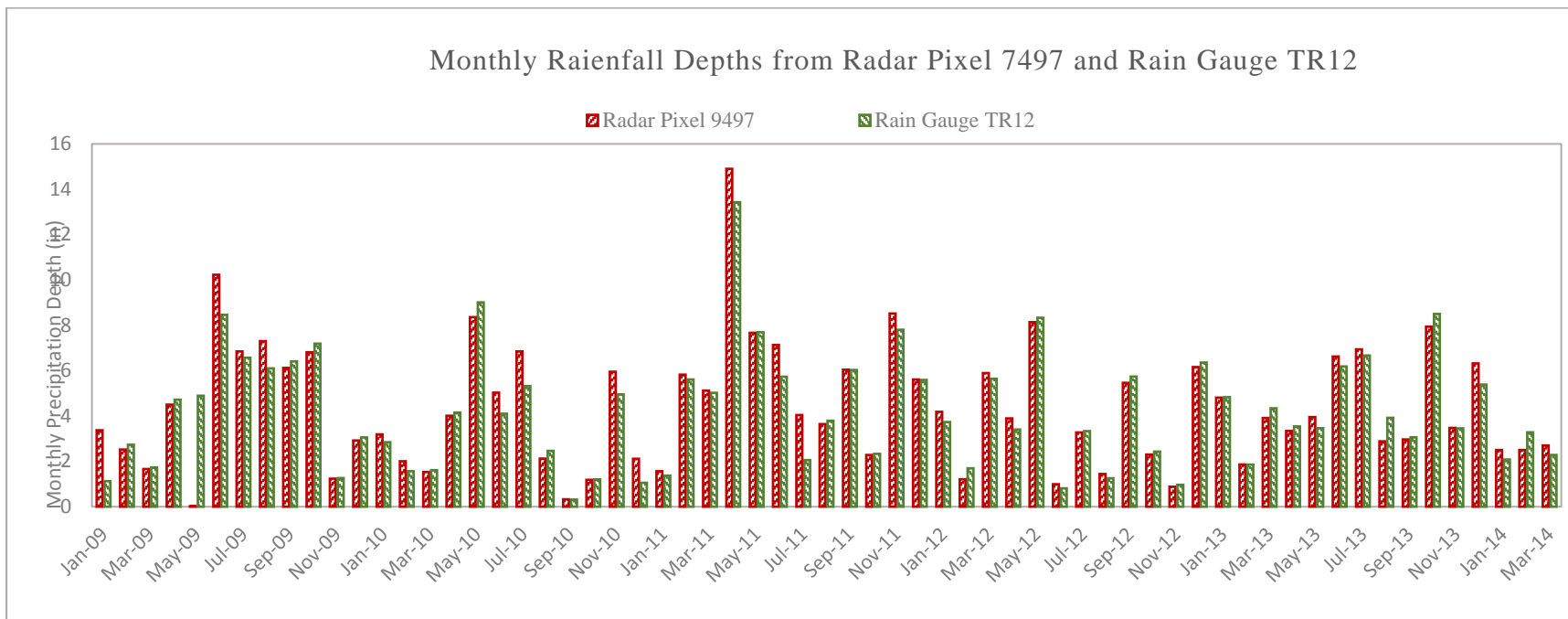


Figure 6. Monthly rainfall Depth form radar pixel 7497 and rain gauge TR12 during January 2009 and March 2014

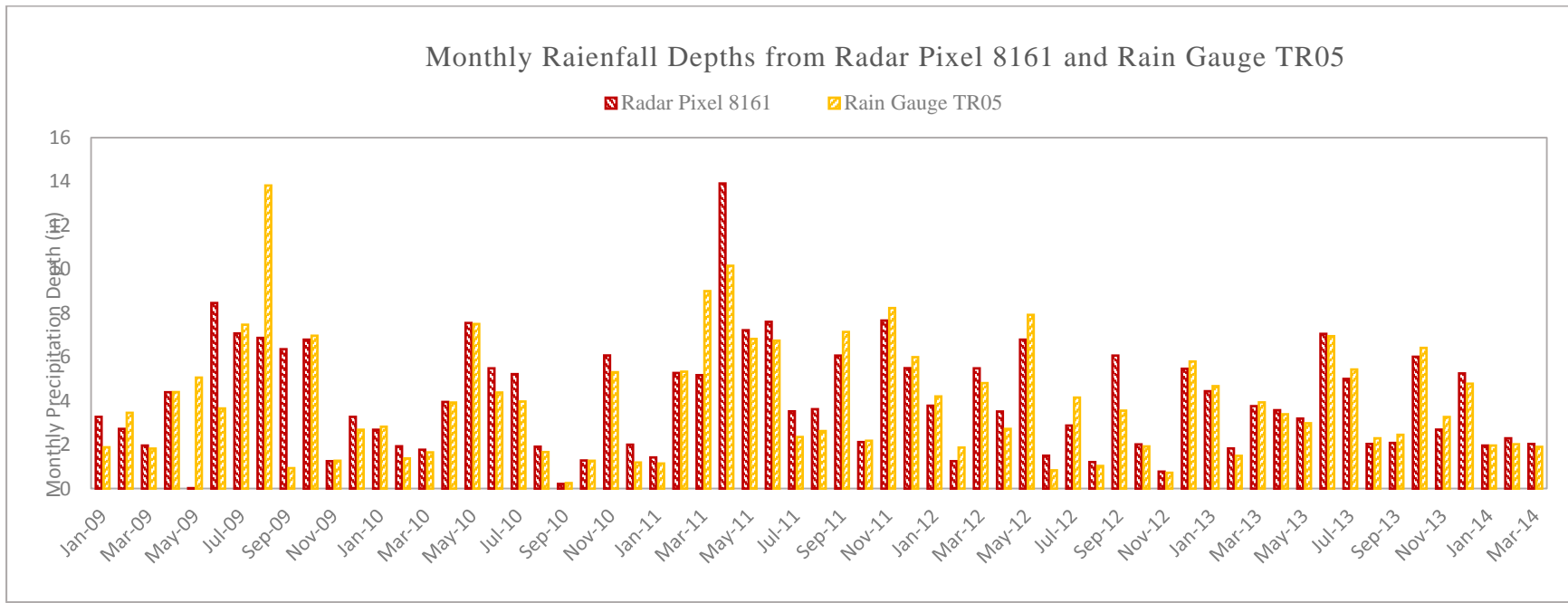


Figure 7 Monthly rainfall Depth form radar pixel 8161 and rain gauge TR05 during January 2009 and March 2014

3.1.2.2 Rainfall Events

Once the radar rainfall data were validated, it is important to subdivide the precipitation data into separate rainfall events. As is defined in the regulations, a ‘representative’ rainfall must yield at least 0.1 inches of precipitation. This is because rainfall depths less than 0.1 inches usually do not produce any measurable runoff (GeoSyntec and ASCE 2002). In this study, the rainfall events were sorted out using 6 hour dry period.

In this section, the radar precipitation data (5 min interval) will be sorted into representative rainfall events according to the following two principles.

- (i) Rainfall depth: at least 0.1 inches
- (ii) Dry period: at least 6 hours

Snow events provide unique challenges when trying to assess rainfall and runoff information. Most importantly, snow has a significant time delay between the event and when it generates runoff. Thus, due to complications and possible errors all the snow events were excluded from the data set by referring to the historical weather record in Louisville. After removing the snow events, 152 rainfall events remained during June 2011 - June 2013, and 43 events for before Jan 2012 (Table 4).

Figure 8 shows the rainfall event took place on June 18th, 2011 in incremental depth (bars) and accumulative depth (curve). The available real-time rainfall record is from June 2011

to June 2013, which include the Pre-BMPs and Post-BMPs rainfall events. Figure 9 shows the real-time rainfall intensity and flow rate during that period.

Table 4

Number of rainfall events pre- and post-installation of the stormwater BMPs

Rainfall Events	Number
Pre-BMPs	43
Post-BMPs	109
Total	152

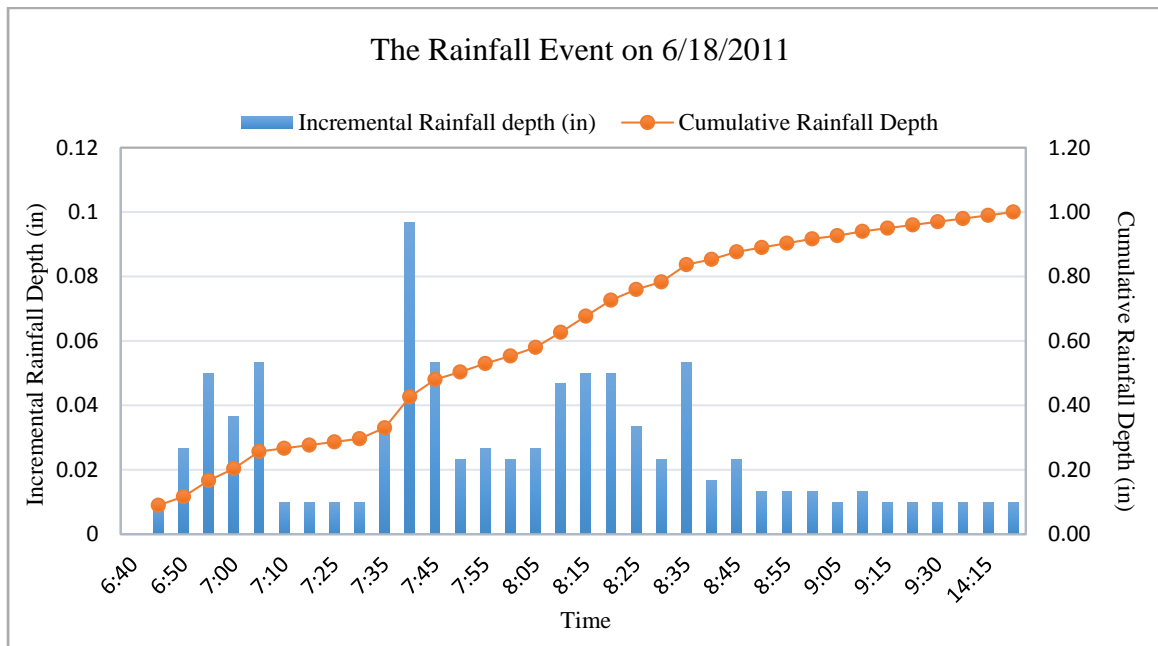


Figure 8. The incremental rainfall depth and the cumulative depth of the rainfall event on 6/18/2011

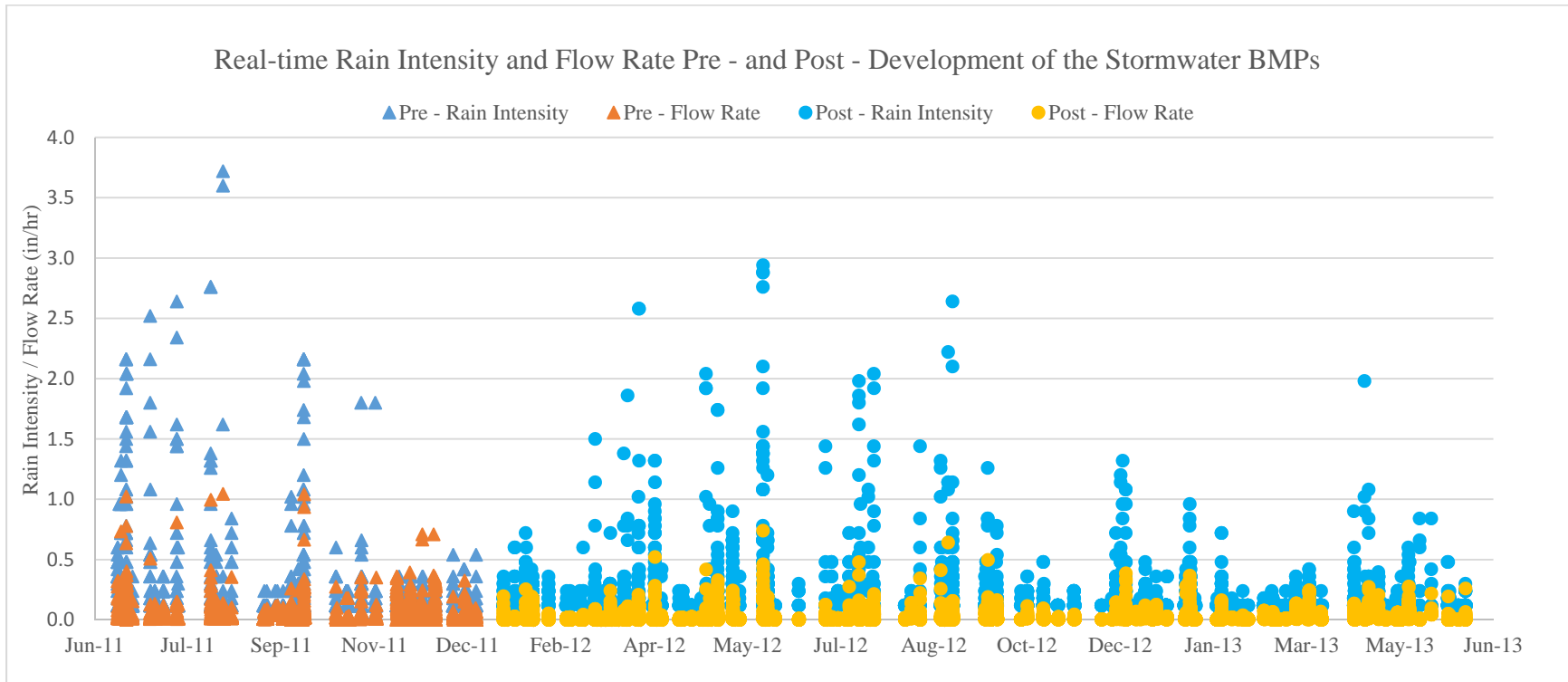


Figure 9. Real-time rainfall intensity and flow rate before and after development of the stormwater BMPs

3.2 Data for Hydraulic Simulation

The combined sewer system was built to convey wastewater to treatment facilities during dry weather conditions, and during wet weather conditions, to also carry stormwater. When a large storm events occur, however, the sewer system reaches capacity, and tends to create overflow, normally called a combined sewer overflow (CSO). The dynamic hydraulic process is simulated by a coupled 1D/2D using XPSWMM.

The data for the coupled 1D/2D hydraulic simulation include rainfall data and hydraulic conditions information, all of which was authorized by Louisville MSD. Two rainfall events were selected to be studied, one of which is a 1-inch rainfall that occurred on June 18, 2011 (Figure 10), and the other is a 4-inch rainfall that occurred on May 29, 2012 (Figure 11).

The information on hydraulic conditions of the study area is compose of land use (Figure 12), topography (Figure 13) and the underground combined sewer system (Figure 14). The land use includes buildings, tree areas, roads, railroads, parking areas, driveways, recreational areas, athletic fields, and grass areas. Figure 13 is a map of contours of the ground elevation for the study area, which has an elevation ranged from 456 ft to 486 ft. Figure 14 shows the study area as a combined sewer watershed, in which the combined sewer drainage route and the outfall location. Flow meter FM0948 is at the outfall location, which means it can measure the flow condition in the combined sewer for the whole study area.

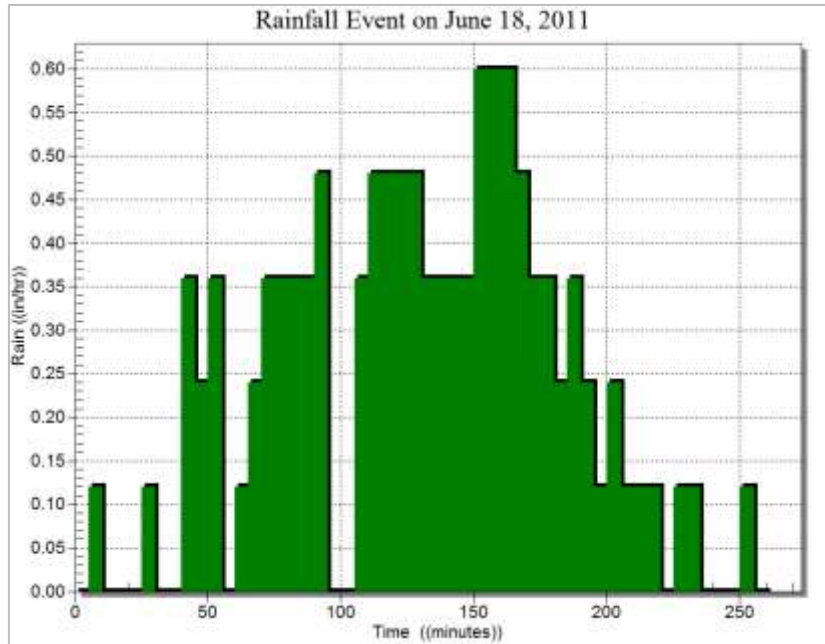


Figure 10 Rainfall event occurred on June 18, 2011

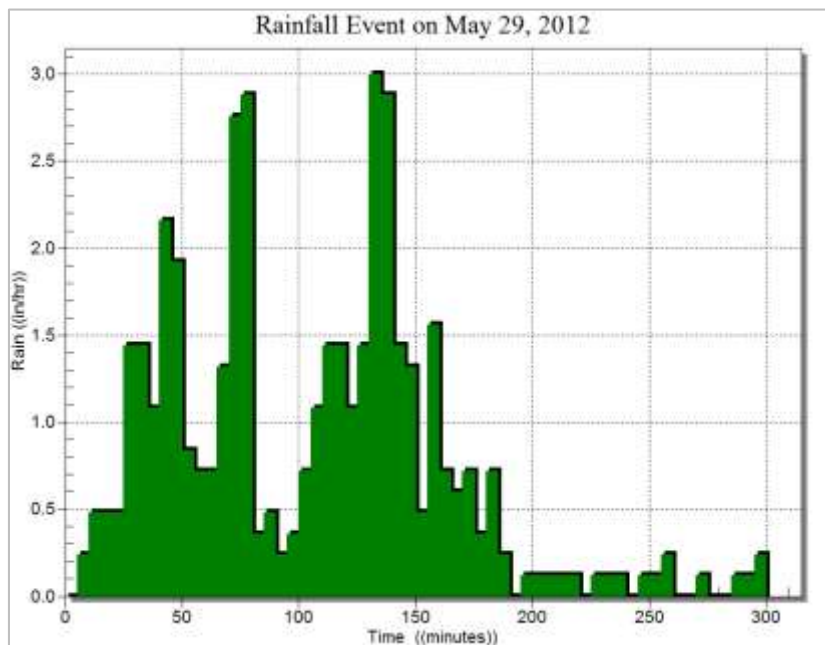
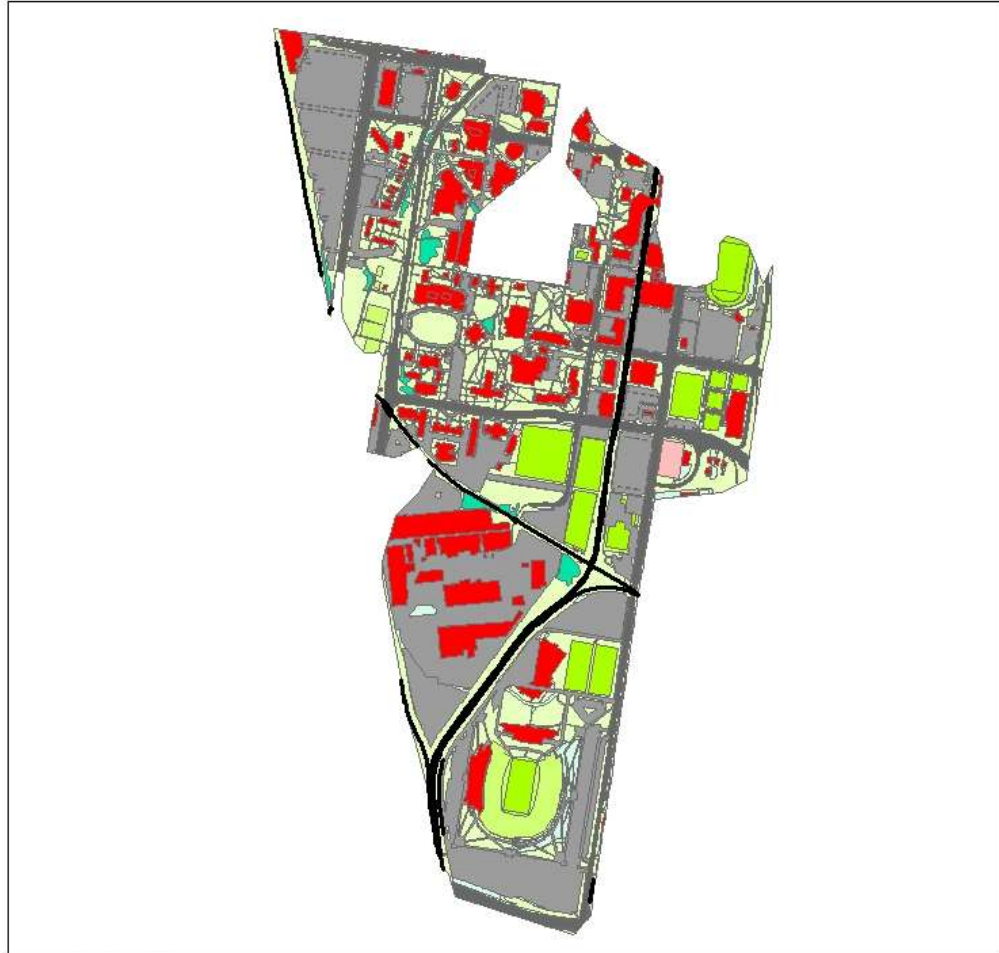


Figure 11 Rainfall event occurred on May 29, 2012

Land Use of the Study Area



- Railroads
- Roads
- Driveway
- Parking
- Athletic Fields
- Recreational Area
- MiscTransportation
- Building
- Tree Area
- Grass



0.04 0.095 0.19 0.285 0.38 Miles



Figure 12 Map of land use for the study area

Contours of the Study Area

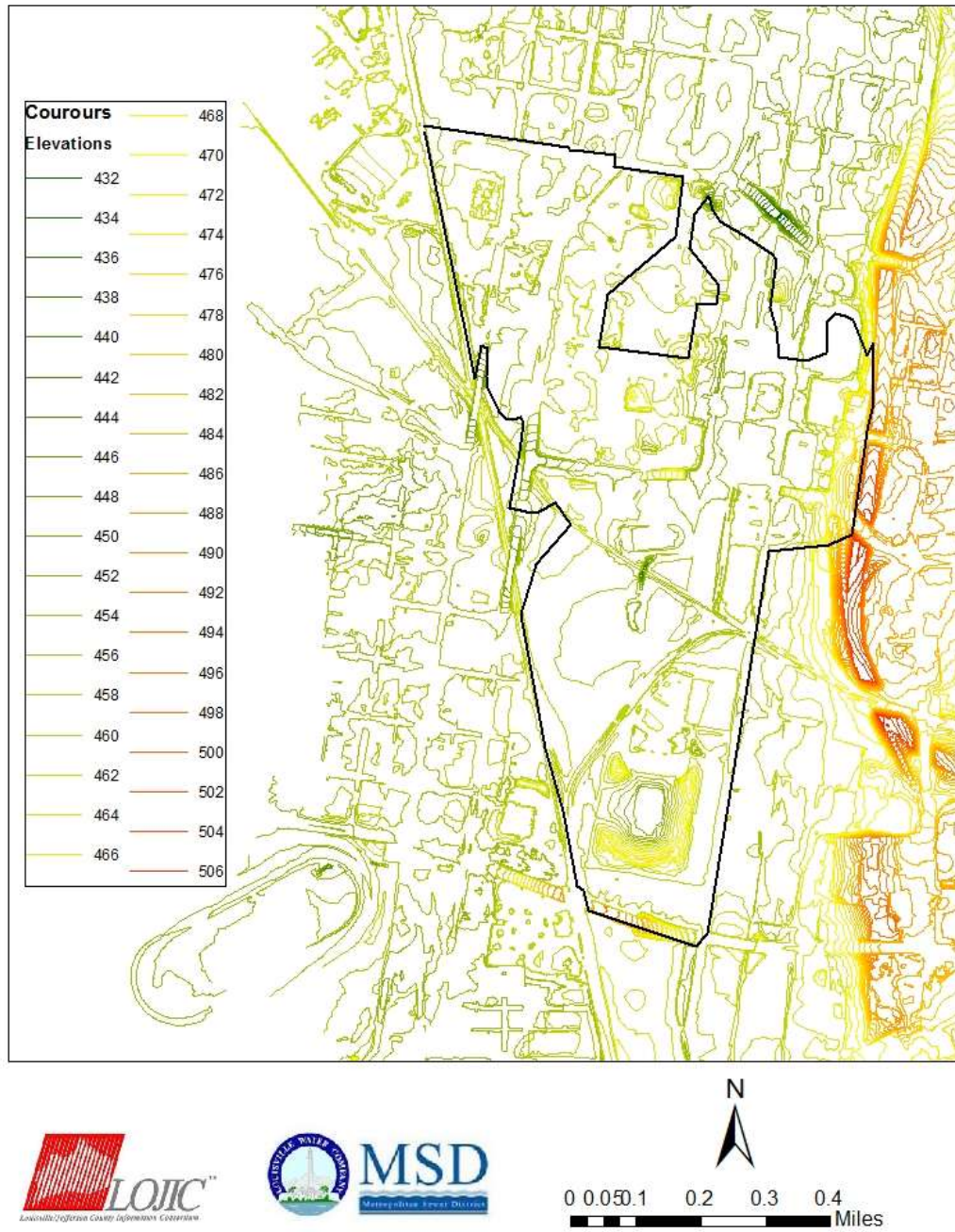


Figure 13 Ground elevation contours of the study area

Sewer System for the Study Area



Legend

-  FM0948
- Sewer Line by Type**
- In Service**
-  Combined
-  CI
-  Sewer
-  Study Area

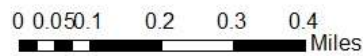


Figure 14 Combined sewer drainage system for the study area

CHAPTER IV

COMPREHENSIVE ASSESSMENT METHODOLOGIES

A comprehensive assessment on the performance of the stormwater BMPs includes evaluations on the changes of magnitudes of flow volume, peak flow, and overflow area. This chapter has two sections: (1) flow volume reduction assessment and peak flow attenuation assessment, and (2) overflow area abatement assessment. The first section presents the assumptions and modelling procedures associated with the rainfall-runoff analysis. The second section discusses the coupled 1D/2D hydraulic simulations for the overflow area.

4.1 Flow Volume Reduction and Peak Flow Attenuation

The development of stormwater BMPs is supposed to change the hydraulic conditions in the study area to promote infiltration and reduce system overflows by alleviating the load of the combined sewer system. Theoretically, the incorporation of BMPs should reduce the flow volume and peak flow in the sewer pipe. However, directly comparing the flow volume or the peak flow before and after the development of stormwater BMPs cannot be exact, because every rainfall has a different pattern.

For example, two rainfall events even with the same overall rainfall depth, may not be comparable because of different durations, different rainfall intensity distributions, or other features that could affect the flow volumes and peak flows. As such, it is necessary to generalize the rainfall features through mining the relationship between rainfall events and the flow volume or peak flows generated by the rainfall events, and then compare the estimated values by the prediction models and real values detected by flow meters.

4.1.1 Proposing Assumption for Modelling

4.1.1.1 Rainfall-Runoff System

The actual physical process that converts rainfall to runoff is both complex and highly variable. The factors affecting runoff are rainfall characteristics/features (depth, intensity, duration, etc.), watershed factors (size, shape, land use, soil type, topography, etc.), meteorology factors (temperature, humidity, wind velocity), and antecedent rainfall conditions (length of dry period). Thus, the amount of stormwater runoff generated by a storm will change as any of the factors change. The question is: what factors should be counted in the rainfall-flow model? What factors can be ignored, and why?

(1) Watershed factors

The watersheds for the study area include only the CSO 211 basin (

Figure 1). As the watershed boundaries and general development conditions within the watershed did not change during the study period, the rainfall-runoff parameters were assumed constant throughout the study. Thus, the watershed factors typically associated with rainfall-runoff calculations have a negligible influence within the models.

(2) Meteorology factors

The amount of runoff tends to be affected by the meteorology factors. For example, high temperature would promote evaporation and transpiration, and low temperature would turn the precipitation into snow, and freeze the runoff. However, the effect of evaporation and transpiration is typically unquantifiable, and usually is ignored in the study of rainfall-runoff system. The snow and freezing events have been excluded in the rainfall data preparation section.

(3) Antecedent rainfall condition

Antecedent rainfall condition refers to the dry period (length of dry weather prior to the storm). Typically, a longer dry period means a better infiltration. In this study, rainfall events were sorted out using a 6 hour dry period, which means 100% of the dry period of the rainfall events is longer than 6 hours. It is also illustrated in Figure 15 that 10% of all the rainfall events has a dry period of less than 12 hours. While, 20% of all the rainfall events has a dry period over 150 hours. Generally, only 30% of the rainfall events fall in the perimeters of extremely wet or extremely dry conditions. Therefore, the effect of

antecedent rainfall condition on the rainfall-runoff system is believed to be little in this study.

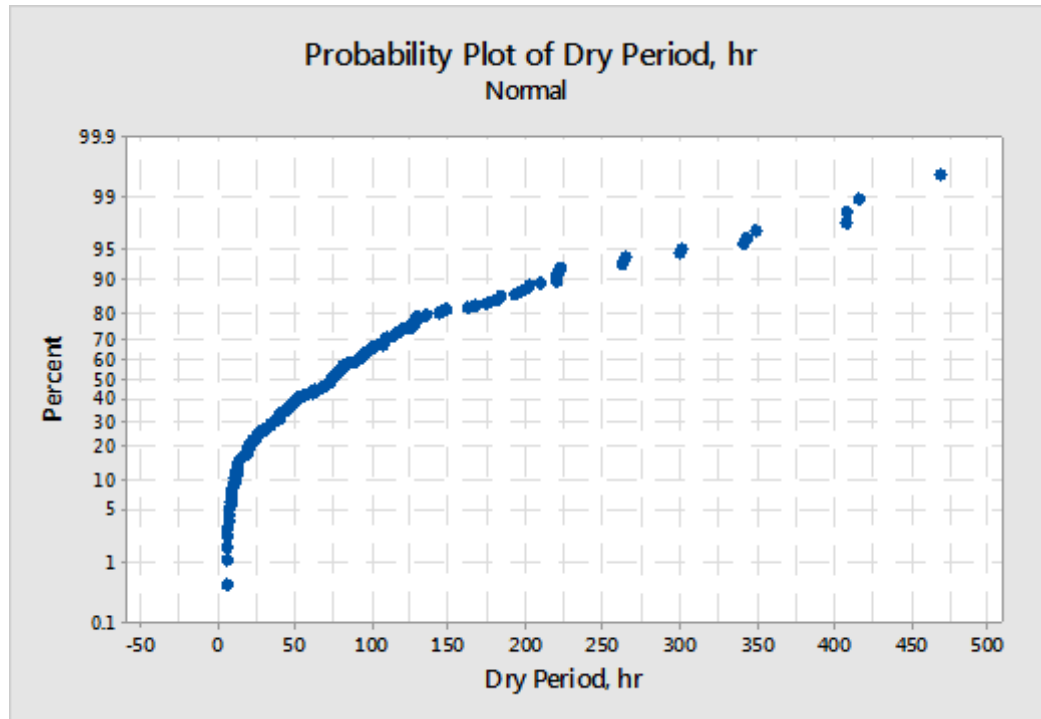


Figure 15. The probability distribution of dry period of the rainfall events

(4) Rainfall characteristics/features

Rainfall depth is defined as the cumulative depth of precipitation in a rainfall event. Rainfall peak intensity is defined as the highest intensity in a rainfall event. These two rainfall features are commonly taken as tied to the flow volume and the peak flow respectively. Presented below is an overview of the important statistical analyses used to

describe rainfall depth and the rainfall peak intensity with respect to either flow volume or peak flow.

Flow Volume

Figure 16 shows the linear relationship between rainfall depth and flow volume. It illustrates that flow volume is closely correlated with rainfall depth with a R^2 of 0.89 (Pre-BMPs) and 0.93 (Post-BMPs) which means that rainfall depth plays an essential role on the magnitude of flow volume. However, when compared to rainfall depth, the peak rainfall intensity seems to be random with the magnitude of flow volume. The R^2 s of the linear expression for peak rainfall intensity and flow volume are 0.04 (Pre-BMPs) and 0.07 (Post-BMPs) respectively (Figure 17). It explains that peak rainfall intensity plays a much less vital role in the magnitude of flow volume.

Peak Flow

Rainfall depth and peak rainfall intensity are also investigated with respect to their effect on peak flow. Figure 18 and Figure 19 illustrate that the R^2 s are ranged from 0.4 to 0.6, which means both rainfall depth and peak rainfall intensity can affect the magnitude of peak flow.

However, what are the most essential rainfall features? Is it possible that both flow volume and peak flow are affected by multiple rainfall features, other than single rainfall feature?

And what are those rainfall features influence on the flow volume or peak flow

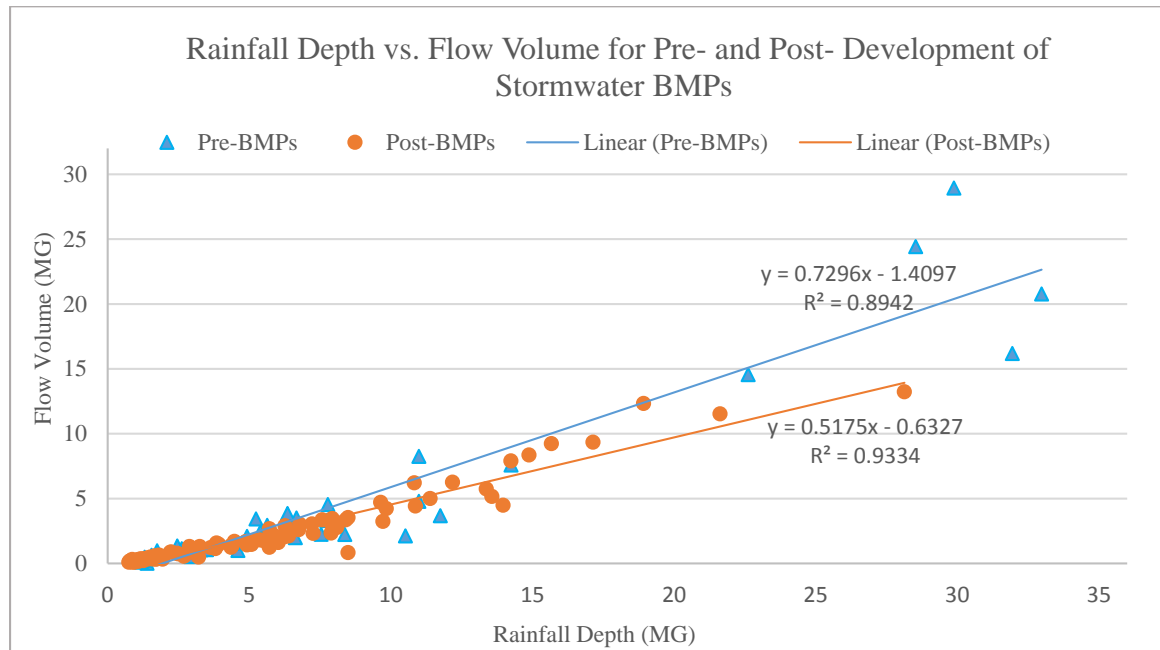


Figure 16. The relationship of flow volume and rainfall depth before and after the installation of stormwater BMPs

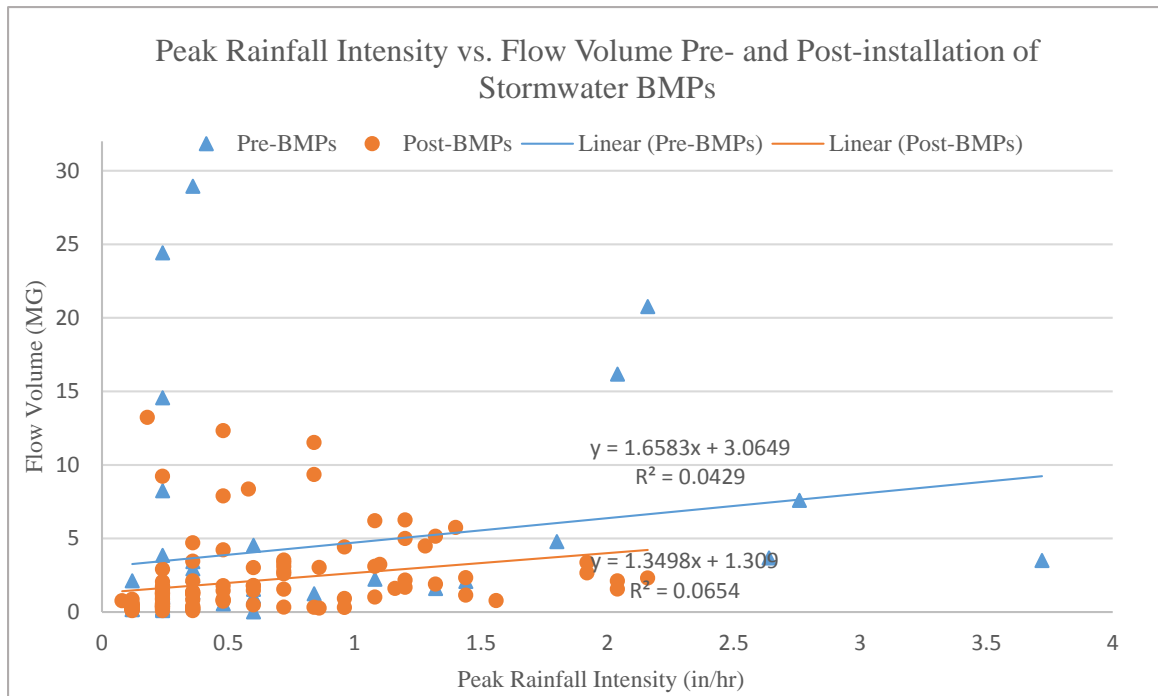


Figure 17. The relationship of flow volume and rainfall depth before and after the installation of stormwater BMPs

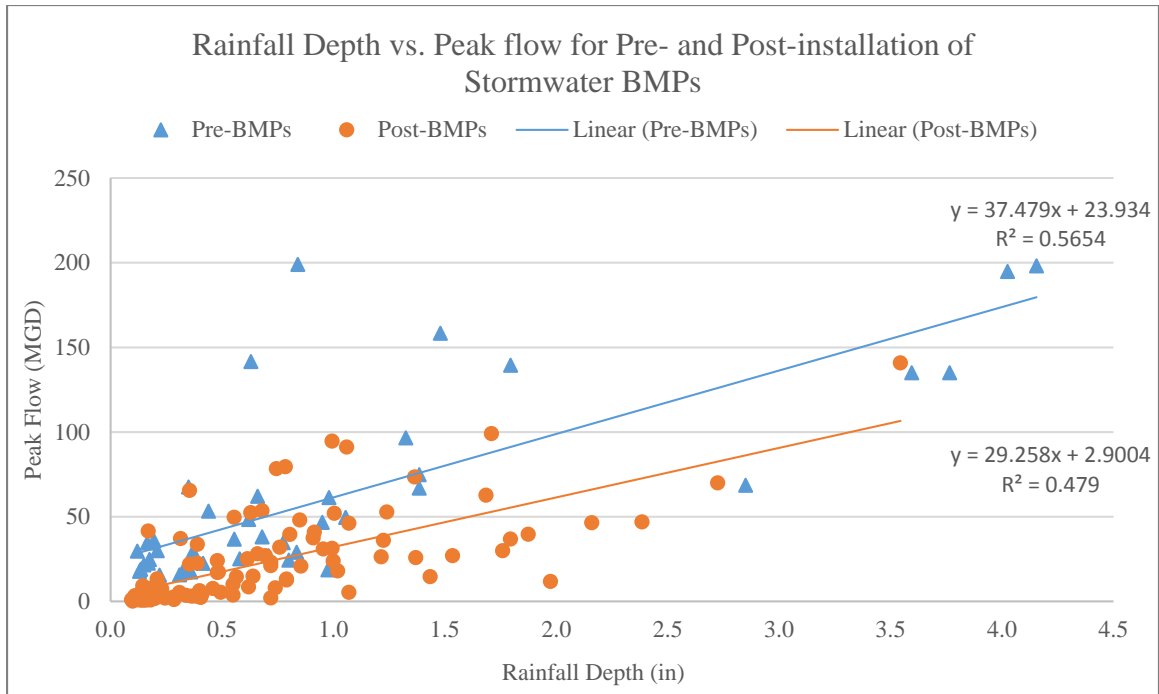


Figure 18. The relationship of flow volume and rainfall depth before and after the installation of stormwater BMPs

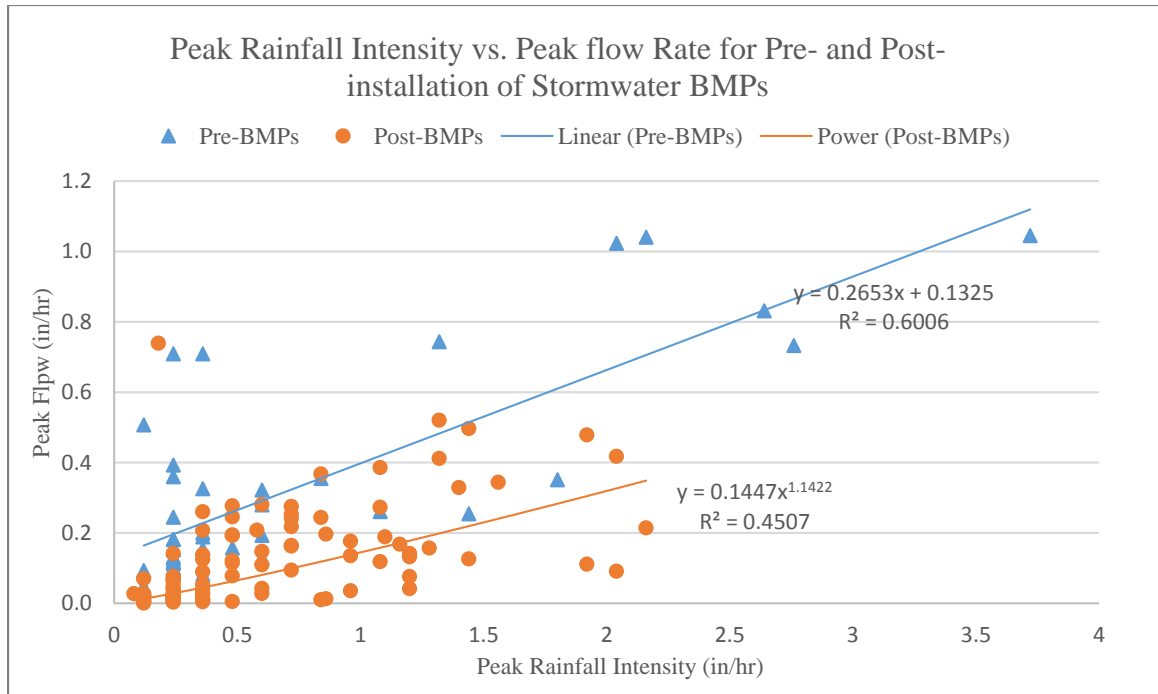


Figure 19. The relationship of peak flow and rainfall depth before and after the installation of stormwater BMPs

4.1.1.2 Assumption

From the above analysis, the effects of watershed factors, and meteorology factors, and antecedent rainfall conditions on the flow (stormwater runoff) could be ruled out, and all the rainfall events could be treated as independent events. Hence, the rainfall features are the sole factor being considered in this study.

The assumptions in this study are:

- (1) All the rainfall events are independent.

(2) The magnitude of the flow volume and/or the peak flow is decided by the features of the rainfall event.

What are the rainfall features we are considering? Take the rainfall event on June 18, 2011 as an example (Figure 20), the rainfall rate and runoff flow rate could be fitted into smooth curves. For the rainfall curve, if the features of rainfall depth, rainfall duration, peak rainfall intensity, time of rising limb, and time of average intensity are fixed, the shape of the curve could be obtained. Those five features are obtained directly from the curve which were defined as direct features. Since the direct features might not be linearly correlated with the magnitude of flow volume or the magnitude of peak flow, some combinations of the feature might be crucial to the accuracy of the model.

Table 5 shows the denotation for the direct rainfall features. The indirect features are generated based on the direct rainfall features. The indirect feature generation process is a dynamic process, and the generating ceases when “desirable” models could be built.

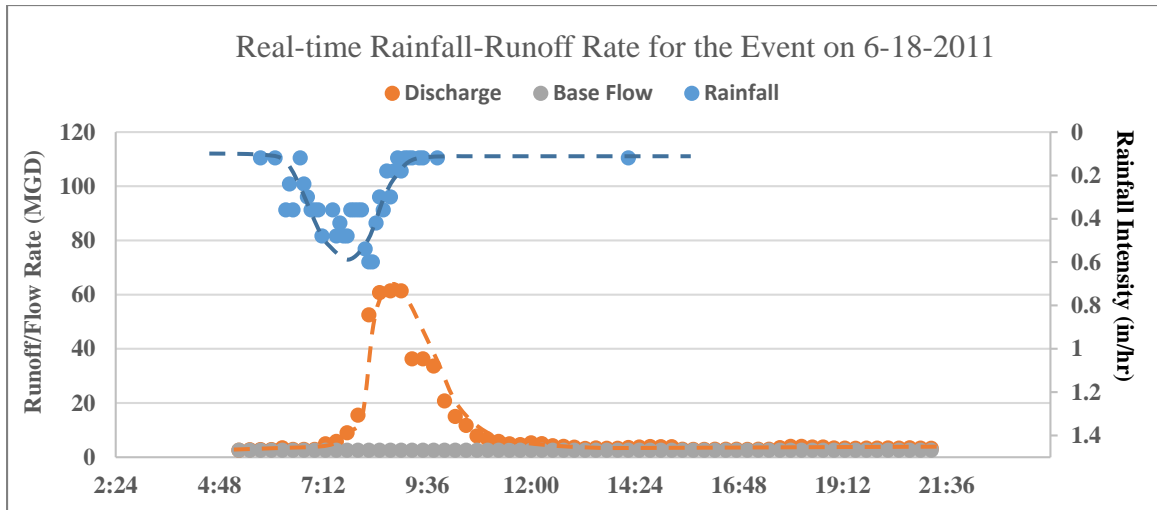


Figure 20. Real-time Rainfall-Runoff Rate for the event on June 18, 2011

Table 5

Denotation for direct rainfall features

D	Depth
T	Duration
i_p	Peak Intensity
t_{rl}	Time of Rising limb
t_{aa}	Time of Above Average Intensity

4.1.2 Modelling Procedures

The assessments on both flow volume reduction and peak flow attenuation are through data mining. The Pre-BMPs rainfall data and detected flow data are used as input and output respectively in the model training and testing phases. When the models are developed, they are used to estimate the magnitude of the flow volume and peak flow for the Post-BMPs rainfall events. The difference of the predicted values and the detected values would be the effect of stormwater BMPs.

As is shown in the flow chart (Figure 21), the data mining procedure starts with standardizing the values of the rain features, and then, choosing the important rainfall features using a feature selection algorithm. Next, develop a multiple linear regression model and an artificial neural network model for each of the rainfall features - flow volume and the rainfall features - peak flow using the Pre-BMPs data. The performance of the stormwater BMPs on flow volume reduction could be obtained through comparing the flow volume estimated by the two models with the actual flow volume detected by the flow meter; the performance of the stormwater BMPs on peak flow could be obtained by comparing the estimated peak flow with the actual detected peak flow.

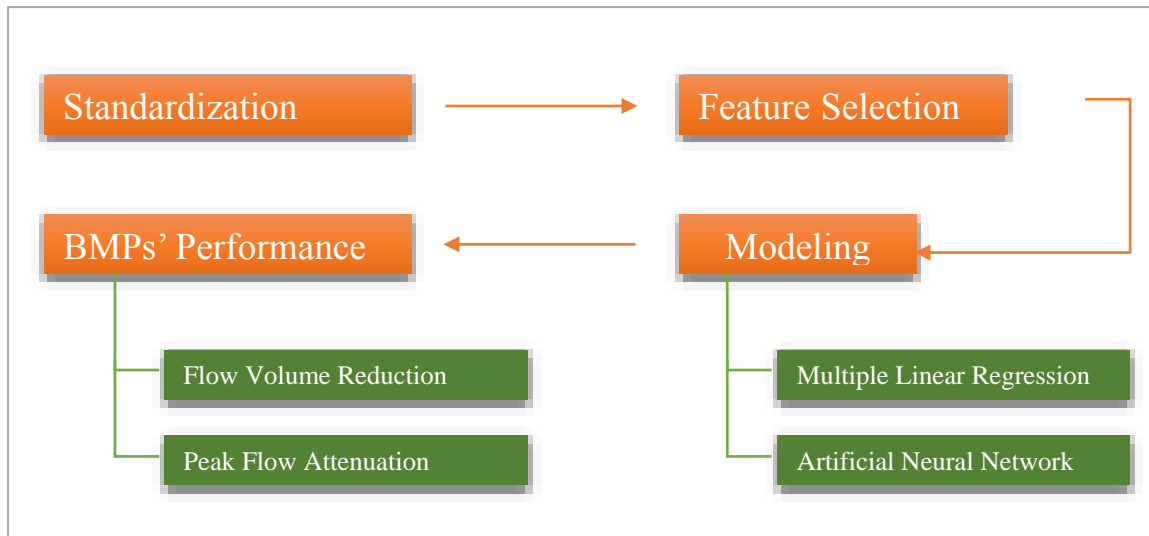


Figure 21. Data mining flow chart

4.1.2.1 Standardization

From the descriptive statistics of the rainfall features in Table 6, it is evident that all the rainfall features are numeric, while at the same time, some rain features have a small range in value, while others have a large range in value. For example, the rainfall depth is ranged in [0.12, 4.16], with a standard deviation of 1.09; while T^2 (square of rainfall duration) is ranged in [1.17, 3471.57], with a standard deviation of 632.31. The large variance between rainfall features in weight will undermine the reliability of the models, and make the model interpretation less meaningful.

Therefore, standardizing the rainfall feature is essential to the following data mining steps. The standardized rainfall feature is obtained from the original rainfall feature divided by the standard deviation, which is shown in the Equation (1).

The descriptive statistics of the rainfall features after standardization are shown in Table 7, in which the values of all the features are between 0 and 7, and the standard deviation for all the features are 1. The weight of all the standardized rainfall features (independent variables) are now on the same order of magnitude.

$$x'_n = \frac{x_n}{\sigma_n} \quad \text{for } n = D, T, i_p, t_{rl}, t_{aa}, \dots; \sigma = \text{Standard Deviation} \quad \dots (1)$$

Table 6

Descriptive Statistics of the Rainfall Features before Standardization

	D	T	i_p	t_{aa}	t_{rl}	D^2	D^3	T^2	$T^{0.5}$	$\ln T$	i_p^2	t_{aa}^2	t_{rl}^2	D/T	$i_p^{0.5}$	$t_{rl}^{0.5}$	D*T	$i_p * t_{rl}$
Max	4.16	58.92	3.72	2.98	39.17	17.31	71.99	3471.57	7.68	4.08	13.84	8.88	1534.29	0.63	1.93	6.26	221.54	15.29
Min	0.12	1.08	0.12	0.08	0.25	0.01	0.00	1.17	1.04	0.08	0.01	0.01	0.06	0.01	0.35	0.50	0.15	0.08
Mean	0.97	12.06	0.69	0.64	4.51	2.10	6.63	291.79	3.12	2.03	1.16	0.98	65.22	0.12	0.74	1.76	19.47	2.27
SD	1.09	12.24	0.83	0.77	6.78	4.47	17.69	632.31	1.55	1.01	2.67	2.05	235.80	0.14	0.40	1.20	43.16	3.66

- 48 -

Table 7

Descriptive Statistics of the Rainfall Features after Standardization

	D	T	i_p	t_{aa}	t_{rl}	D^2	D^3	T^2	$T^{0.5}$	$\ln T$	i_p^2	t_{aa}^2	t_{rl}^2	D/T	$i_p^{0.5}$	$t_{rl}^{0.5}$	D*T	$i_p * t_{rl}$
Max	3.82	4.81	4.48	3.87	5.78	3.87	4.07	5.49	4.95	4.04	5.18	4.33	6.51	4.51	4.82	5.22	5.13	4.18
Min	0.11	0.09	0.14	0.10	0.04	0.00	0.00	0.00	0.67	0.08	0.01	0.00	0.00	0.07	0.87	0.42	0.00	0.02
Mean	0.89	0.99	0.84	0.83	0.66	0.47	0.37	0.46	2.01	2.01	0.43	0.48	0.28	0.87	1.84	1.47	0.45	0.62
SD	1.00	1.00	1.00	1.00	1.00	1.00	1.00	1.00	1.00	1.00	1.00	1.00	1.00	0.99	0.99	1.00	1.00	1.00

4.1.2.2 Feature Selection

Feature selection, also known as attribute selection, is the process of selecting a subset of relevant features for use in model construction (Yang and Pedersen 1997, Guyon and Elisseeff 2003). Weka, a data mining software in Java, was employed to practice feature selection. The evaluator used is CfsSubsetEval, which evaluates the worth of a subset of attributes by considering the individual predictive ability of each feature along with the degree of redundancy between them (Kittler 1986, Hall, Frank et al. 2009). Subsets of features that are highly correlated with the class while having low inter-correlation are preferred (Hall 1999). The search method used in this study is best first, which searches the space of attributes subsets by greedy hill-climbing algorithm (a mathematical optimization technique) which augmented with a back-tracking facility (Hall, Frank et al. 2009), and the search direction is forward (Guyon, Andr et al. 2003).

The standardized rainfall features are used in the feature selection. Figure 22 and Figure 23 are the interface feature selection results on Weka for flow volume and peak flow respectively. The selected features are listed in Table 8. The selected rainfall features for flow volume are rainfall depth, rainfall depth cubic, and the product of rainfall depth and rainfall duration. The selected rainfall features for peak flow are rainfall depth, peak rainfall intensity, duration of above average intensity, and average rainfall intensity.

Table 8

Important Rainfall Features Affecting Flow Volume and Peak Flow

	Selected Features			
Flow Volum (Fv)	D	D ³	D×T	
Peak Flow (Fp)	D	i _p	t _{aa}	D/T

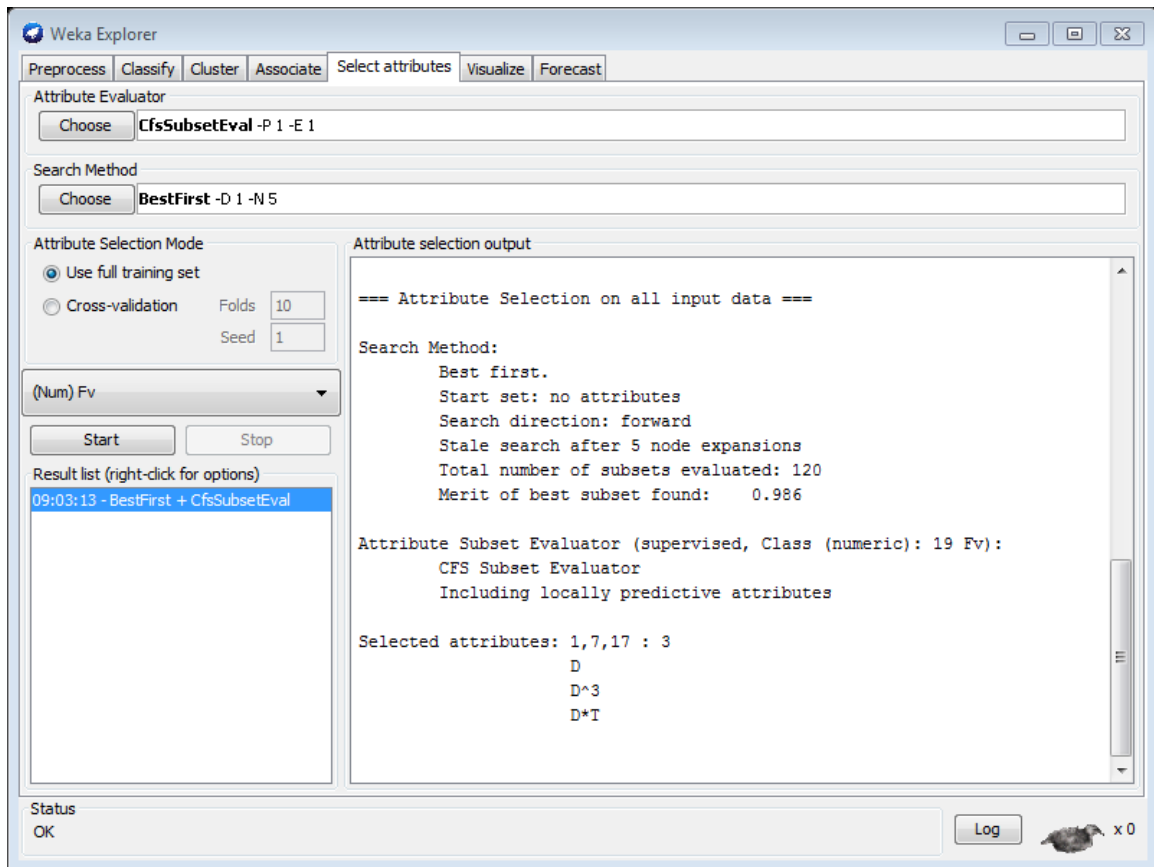


Figure 22. Result of rainfall feature selection for flow volume on Weka

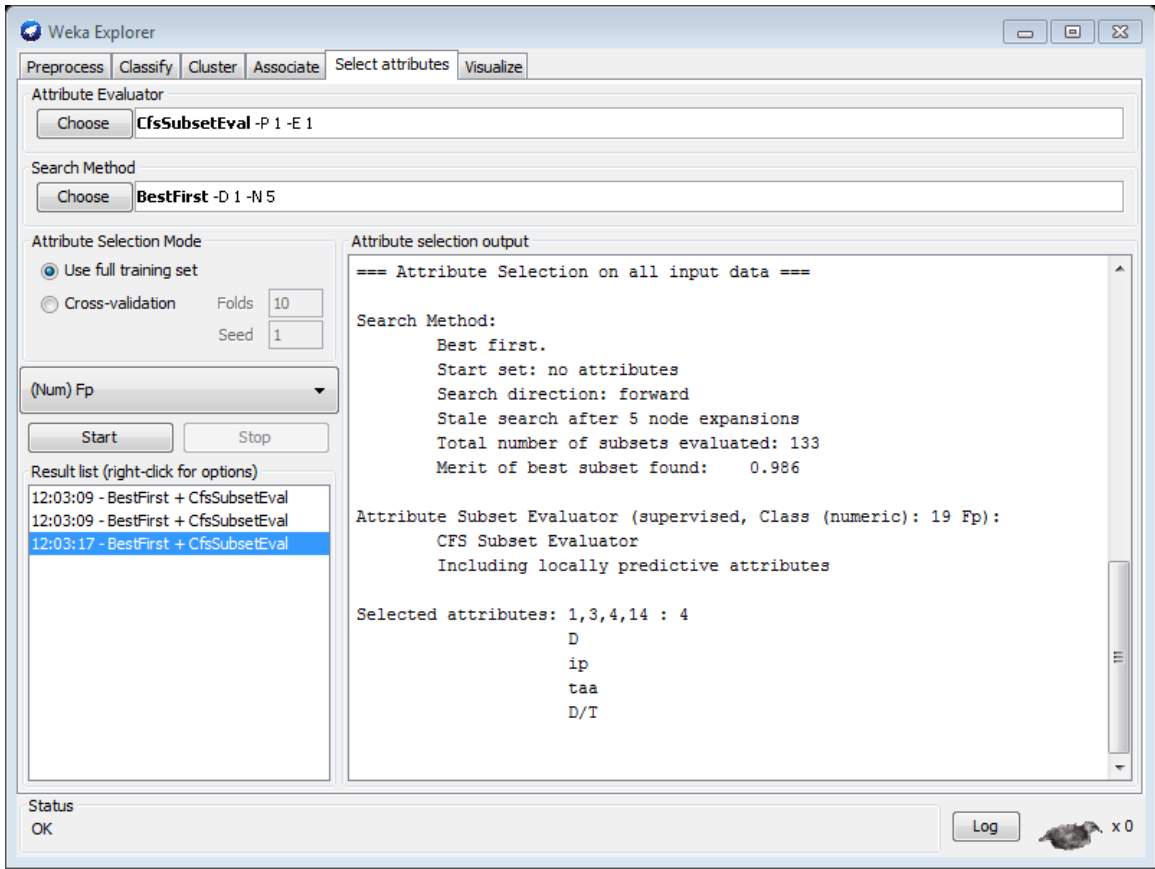


Figure 23. Result of rainfall feature selection for peak flow on Weka

4.1.2.3 Multiple Linear Regression Model

Two Multiple Linear Regression Models (MLRMs) were built in this section, one is for rainfall - flow volume, and the other one is for rainfall - peak flow. In the rainfall – flow volume model, the independent variables are the selected rainfall features for flow volume; in the rainfall – peak flow model, the independent variables are the selected rainfall features for peak flow. The flow volume MLRM and the peak flow MLRM were built, and the expression of which are shown in equation (2) and equation (3).

Flow Volume (Fv)

$$Fv = -0.06 + 2.79D + 1.38 D^3 + 2.92 D \cdot T \quad \dots \dots \quad (2)$$

The Adj R² (adjusted square of multiple correlation from the regression) is 0.96 (Table 9), which means 96% of variation of flow volume could be explained by rainfall depth, cubic of rainfall depth, and the product of rainfall depth and rainfall duration (Li, Zhang et al. 2014). Table 10 shows the analysis of the coefficients in the flow volume MLRM. The P-Value of all the independent variables are ca. 0.00 (<< 0.05), indicating each of the selected rainfall features has a significant contribution to the flow volume (Fox 1991).

It is very clear that in the study area, rainfall depth is the most important feature, followed by rainfall duration. The flow volume in the combined sewer can grow exponentially with rainfall depth.

Table 9

Fit-of-goodness for Flow Volume MLRM

S	R ²	R ² (adj)	R ² (pred)
11.6184	96.34%	95.96%	91.80%

Table 10

Analysis of Coefficients for Flow Volume MLRM

Source	DF	Adj SS	Adj MS	F-Value	P-Value
Regression	3	1825.25	608.416	590.03	0.000
D	1	37.45	37.452	36.32	0.000
D ³	1	10.97	10.965	10.63	0.002
D·T	1	148.91	148.911	144.41	0.000
Error	39	40.22	1.031	70.99	0.014
Total	42	1865.46			

(DF denotes degree of freedom, Adj SS denotes adjusted sum of square, Adj MS denotes mean square of error)

Since one of the most important assumptions of the regression model is the residual (estimated error) is random, which means it is from normal distribution (Osborne and Waters 2002). A normality test for the residuals was made and the results shown in Figure

24. We could see the P-Value of the normality test for the flow volume MRLM is 0.09 (> 0.05), indicating the residual is from normal distribution.

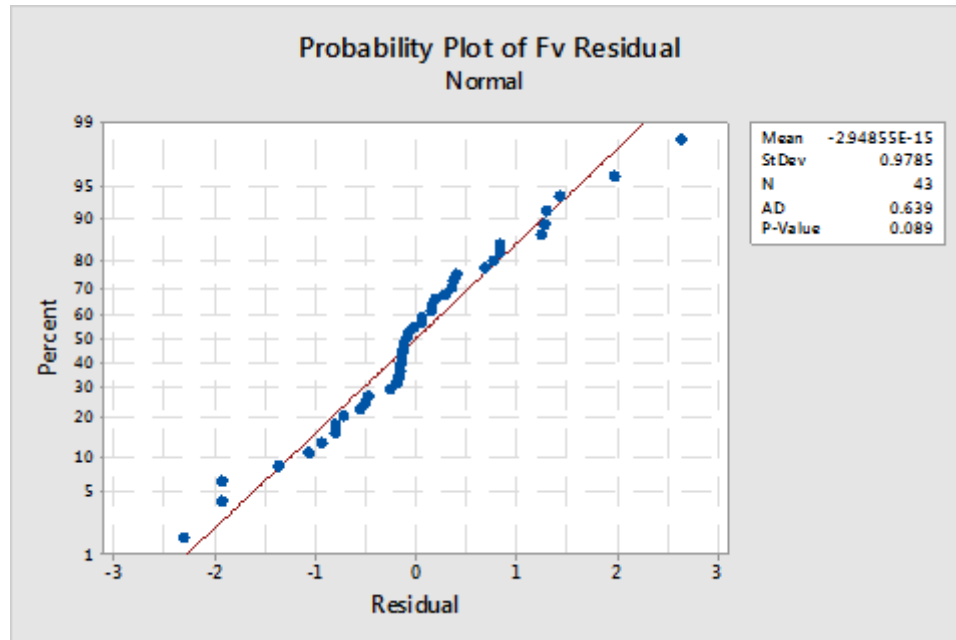


Figure 24. Normality test for the flow volume MLRM

Peak Flow (Fp)

$$Fp = 3.61 + 18.17D + 7.9i_p + 15.60t_{aa} + \frac{24.96D}{T} \dots\dots (3)$$

The Adj R² is 0.98 (Table 11), which means 98% of variation of peak flow could be explained by rainfall depth, peak rainfall intensity, time of above average rainfall intensity, and the average rainfall intensity (rainfall depth divided by rainfall duration). Table 12 show the analysis of the coefficients in the peak flow MLRM. The P-Value of all the independent variables are ca. 0.00 (<< 0.05), indicating each of the selected rainfall features has a significant contribution to the peak flow.

It shows that in the study area, the peak flow is decided by rainfall depth, peak rainfall intensity, duration and duration of above average rainfall intensity. Peak flow is negatively correlated with rainfall duration, while positively correlated with other three features.

Table 11

Fit-of-goodness for Peak Flow MLRM

S	R ²	R ² (adj)	R ² (pred)
7.22306	98.40%	98.23%	97.09%

Table 12

Analysis of Coefficients for Peak Flow MLRM

Source	DF	Adj SS	Adj MS	F-Value	P-Value
Regression	4	121622	30405.4	582.79	0.000
D	1	7209	7208.8	138.17	0.000
i _p	1	883	882.6	16.92	0.000
t _{aa}	1	4606	4605.8	88.28	0.000
D/T	1	8771	8770.6	168.11	0.000
Error	38	1983	52.2		
Total	42	123604			

(DF denotes degree of freedom, Adj SS denotes adjusted sum of square, Adj MS denotes mean square of error)

A normality test for the residuals also was made for peak flow MLRM, and the results are shown in Figure 26. The P-Value of the normality test is 0.11 (> 0.05), indicating the residuals is from normal distribution.

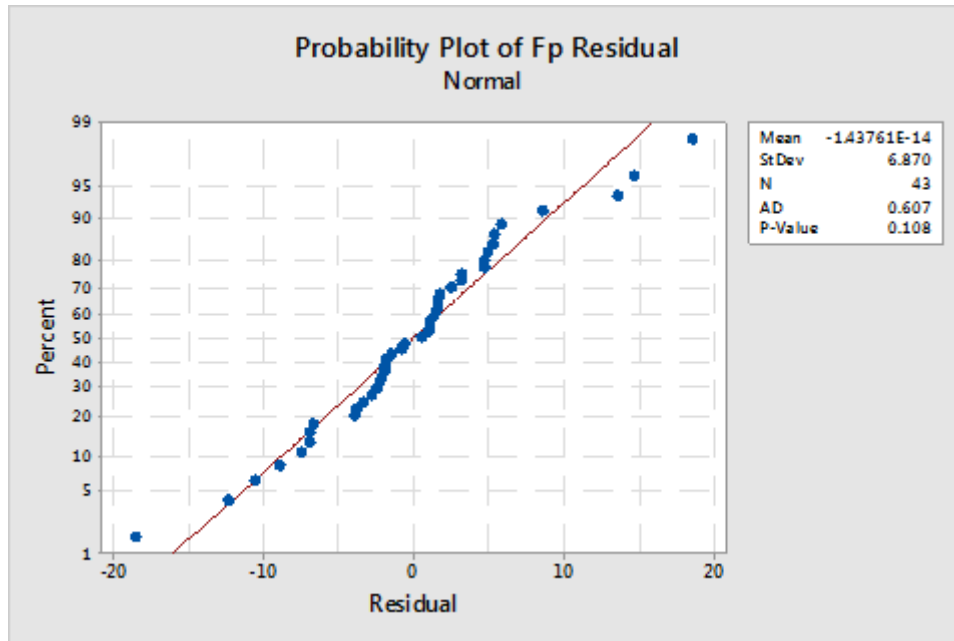


Figure 25. Normality test for the peak flow MLRM

4.1.2.4 Artificial Neural Network Model

Artificial neural network was also applied to build the rainfall features - flow volume model, and the rainfall features - peak flow model using the selected rainfall features. The training algorithm employed is back propagation which is a supervised learning algorithm. Two Back Propagation Neural Network Models (BPNNM) were built in this section.

In splitting data for training and testing, 10 fold cross-validation was applied (Kohavi 1995). It partitions the training set into 10 subsets. For each model complexity, the learner trains 10 times, each using one of the sets as the validation set and the remaining sets as the training set. It then selects the model complexity that has the smallest average error on the validation set (Krogh and Vedelsby 1995).

Learning rate and momentum are important factors in adjusting neurons' weight. Learning rate (a decreasing function of time) scales the derivative, and has an important effect on the time needed until convergence is reached. Momentum scales the influence of the previous step on the current, which is supposed to make the learning procedure more stable and accelerate convergence of the error function (Riedmiller and Braun 1993). The learning rate is used as a fixed value, ranging from 0 to 1. The smaller the learning rate, the smaller the residual deviation but the slower the convergence rate (Chinrungrueng and Sequin 1995). The value of the momentum should be also in between 0 and 1. Since we have three independent variables for the flow volume BPNNM, and four independent variables for the peak flow BPNNM, the number of neural nodes is considered to choose from 0 to 4.

In spite of the mean absolute error, root mean square error, and relative absolute error, the correlation coefficient is the most important factor in indicating the stability and reliability of the neural network model. It is found that the correlation coefficient changes with different settings on learning rate, momentum, and number of nodes. The question is: how to obtain the highest correlation coefficient by setting up these factors? Let's see how the single factor affects the correlation coefficient.

Figure 26 and Figure 27 illustrate that the correlation coefficient fluctuates with the learning rate, and the correlation coefficient is a maximum when the learning rate is 0.1 both for the flow volume BPNNM (correlation coefficient = 0.86) and peak flow BPNNM (correlation coefficient = 0.86). For the momentum, the correlation coefficient decreases with its growing. Therefore, the correlation coefficients (0.92 for flow volume BPNNM, 0.96 peak flow BPNNM) are highest when the momentum is set up as 0. For the number of hidden nodes, 2 hidden nodes will maximize the correlation coefficient of flow volume BPNNM, and 3 hidden nodes will maximize the correlation coefficient of peak flow BPNNM. The above analysis is focusing on single factors, which means other factors are fixed when considering the specific factor.

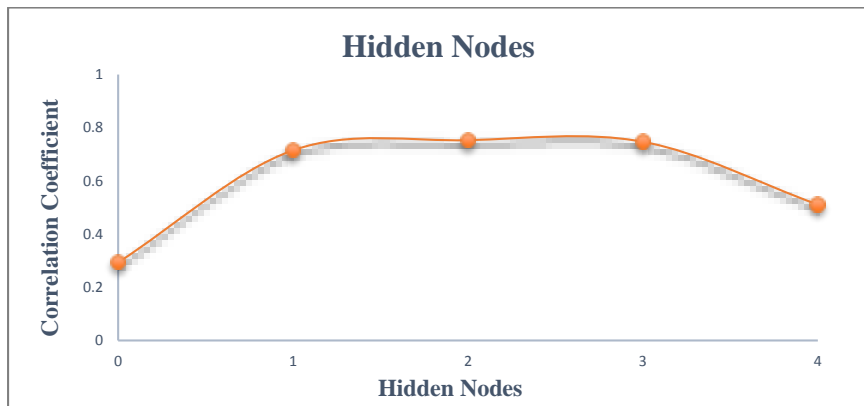
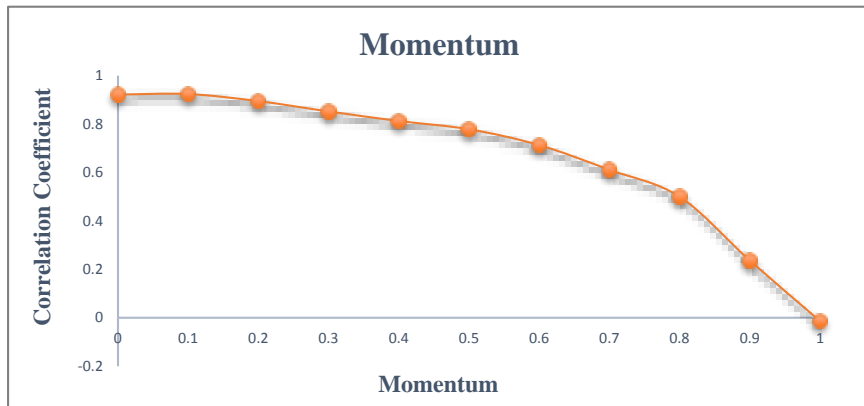
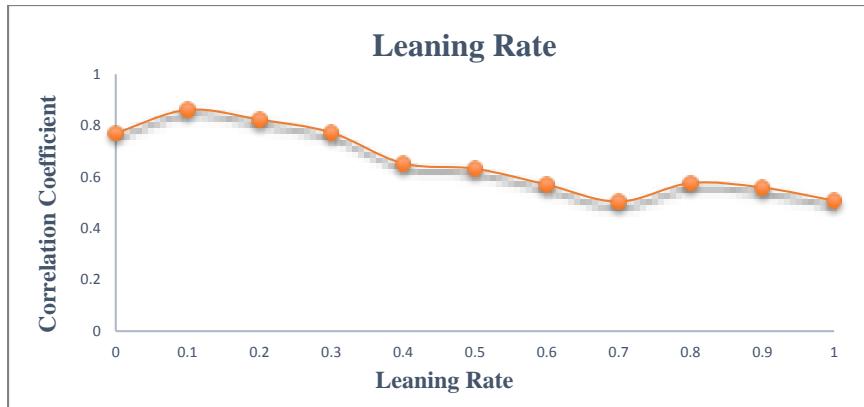


Figure 26. Correlation coefficients of the flow volume BPNNM with the change of learning rates, momentums, and hidden nodes

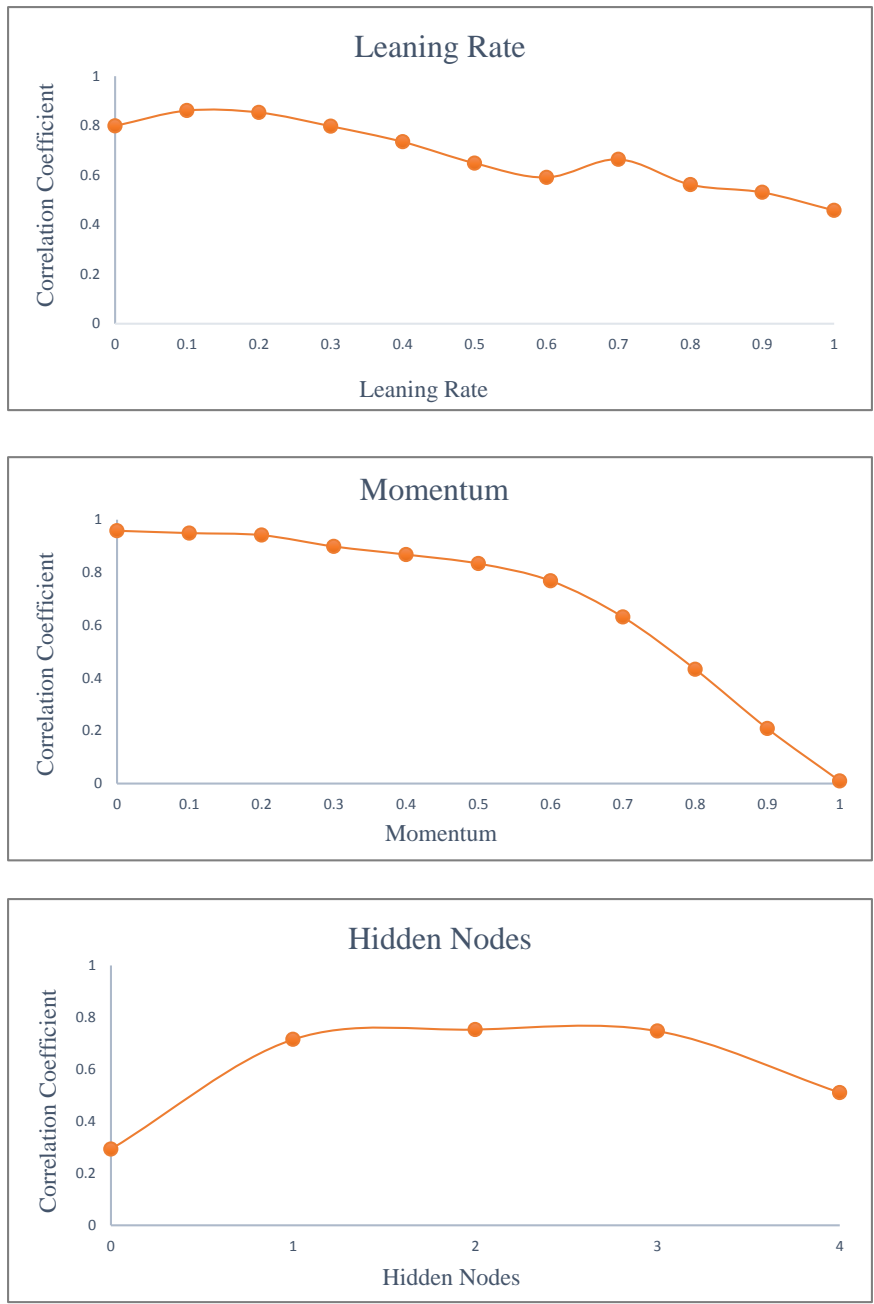


Figure 27. Correlation coefficients of the peak flow BPNNM with the change of learning rates, momentums, and hidden nodes

From the above analysis, the variation trend of the model's correlation coefficient is clearly shown. However, in search for the optimal combination of the learning rate, momentum, and number of nodes, a full factorial experiment was performed. The value range for both learning rate and momentum are both set as [0, 1] with the step of 0.1, and the number of nodes is ranged at [0, 4] with the step of 1, which make the total number of combinations of all those choices 605 for each BPNNM.

To accelerate the searching process, a program was written in Java language to find the optimal combination of learning rate, momentum, and number of nodes for correlation coefficient (see Appendix). The program can call the MultilayerPerceptron algorithm in Weka (Hall, Frank et al. 2009). The optimal combination for flow volume BPNNM and peak flow BPNNM are shown below.

Flow volume BPNNM

The optimal combination of the learning rate, momentum, and number of nodes flow volume BPNNM is 0.3, 0.5, and 4 respectively (Figure 28). The running results are shown in Table 13. The maximum correlation coefficient of the model is 0.98.

Table 13

Flow Volume BPNNM Running Result

=== Run information ===

Scheme: weka.classifiers.functions.MultilayerPerceptron -L 0.3 -M 0.5 -N 500 -V 0 -S 0 -E 20 -H 4
Relation: Pre-BMPs-weka.filters.unsupervised.attribute.Remove-R2-6,8-16,18-19
Instances: 43
Attributes: 4 (D, D3, D*T, Fv)
Test mode: 10-fold cross-validation

=== Classifier model (full training set) ===

Linear Node 0

Inputs	Weights
Threshold	-0.5380423623357347
Node 1	0.16605206954100468
Node 2	1.5947754319284373
Node 3	0.19342328454059918
Node 4	-0.9419784293085267

Sigmoid Node 1

Inputs	Weights
Threshold	-1.0078681562602674
Attrib D	0.3780623051212866
Attrib D3	0.5499326755567432
Attrib D*T	0.6500223809013068

Sigmoid Node 2

Inputs	Weights
Threshold	-0.7302148990886627
Attrib D	0.8309811412055409
Attrib D3	0.9540482142716712
Attrib D*T	1.818236612109338

Sigmoid Node 3

Inputs	Weights
Threshold	-0.9904640330903244
Attrib D	0.40843625105534453
Attrib D3	0.5513880759374299
Attrib D*T	0.6498527608147631

Sigmoid Node 4

Inputs	Weights
Threshold	-1.5636109773970421
Attrib D	-2.1396932318708433
Attrib D3	0.4028818101003671

	Attrib D*T	0.12882026997754897
Class	Input	
	Node 0	
Time taken to build model: 0.17 seconds		
==== Cross-validation ====		
==== Summary ====		
Correlation coefficient		0.9769
Mean absolute error		1.3062
Root mean squared error		2.0045
Relative absolute error		29.5543 %
Root relative squared error		29.4494 %
Total Number of Instances		43

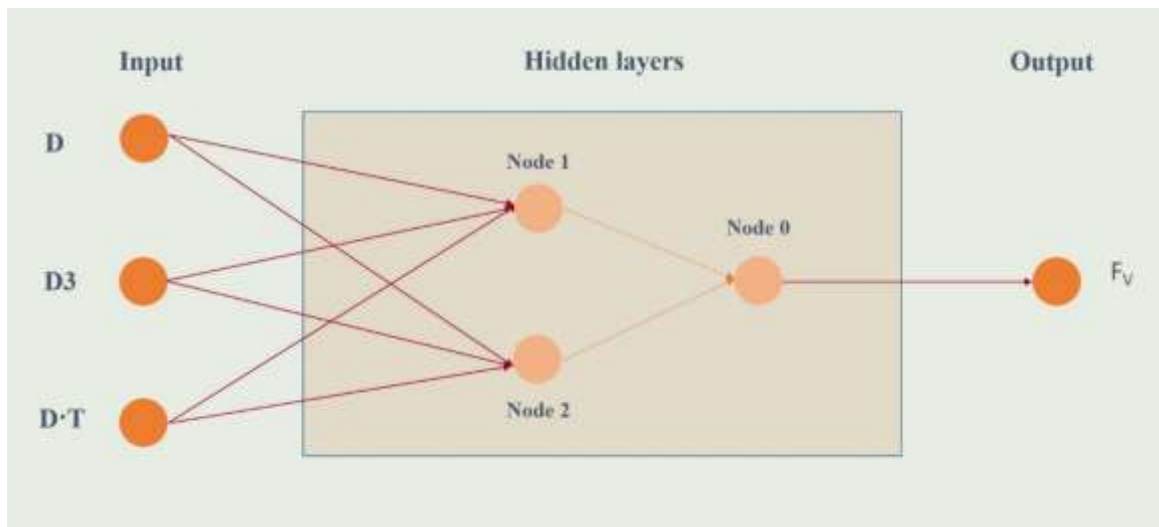


Figure 28. The structure of flow volume BPNN

Peak flow BPNNM

The optimal combination of the learning rate, momentum, and number of nodes peak flow BPNNM is 0.1, 0, and 2 respectively (Figure 29). The running result is shown in Table 14.

The maximum correlation coefficient of the model is 0.99.

Table 14

Peak Flow BPNNM Running Result

=== Run information ===

Scheme: weka.classifiers.functions.MultilayerPerceptron -L 0.1 -M 0.0 -N 500 -V 0 -S 0 -E 20 -H 2

Relation: Pre-BMPs-weka.filters.unsupervised.attribute.Remove-R2,5-13,15-18,20

Instances: 43

Attributes: 5 (D, ip, taa, D/T, Fp)

Test mode: 10-fold cross-validation

=== Classifier model (full training set) ===

Linear Node 0

Inputs	Weights
Threshold	1.3146414557907469
Node 1	-0.9293701228309864
Node 2	-1.8920564928053003

Sigmoid Node 1

Inputs	Weights
Threshold	-0.41172891145727053
Attrib D	-0.3776188802813853
Attrib ip	-0.2868179790252736
Attrib taa	0.0799960892446779
Attrib D/T	-0.7926666399101188

Sigmoid Node 2

Inputs	Weights
Threshold	-1.340853557859408
Attrib D	-0.7976832711339032
Attrib ip	-0.3847935160005908

	Attrib taa	-0.8543145877606572
	Attrib D/T	-1.1280006130867009
Class	Input	Node 0

Time taken to build model: 0.14 seconds

==== Cross-validation ====

==== Summary ====

Correlation coefficient	0.9878
Mean absolute error	6.4459
Root mean squared error	8.3583
Relative absolute error	15.1678 %
Root relative squared error	15.3407 %
Total Number of Instances	43

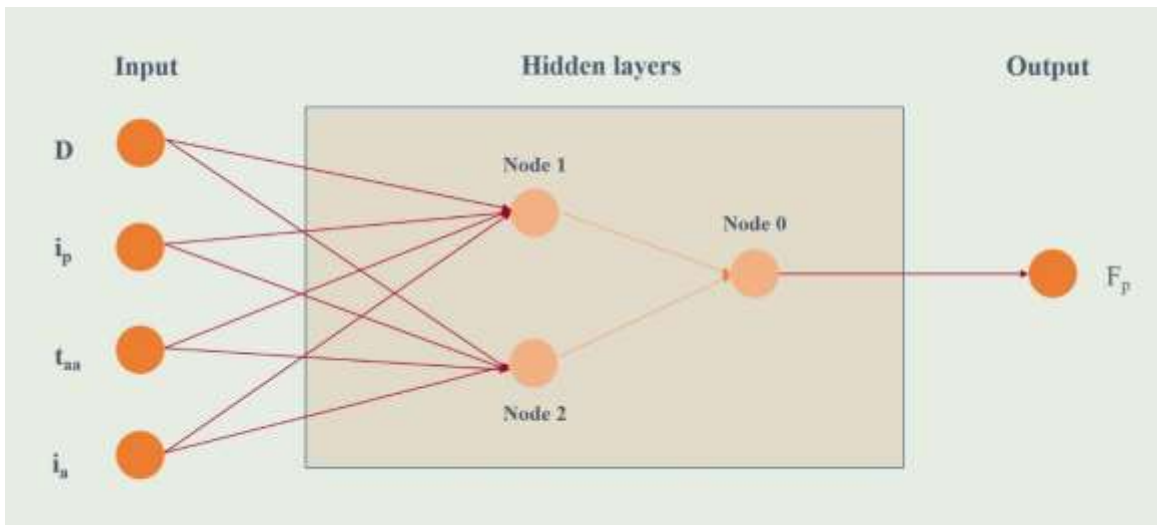


Figure 29. The structure of peak flow BPNNM

4.1.2.5 Design Parameters

The design parameters of the stormwater BMPs could also be used to estimate the stormwater flow volume reduction using their designed storage capacities. It could be considered as an additional method in assessing the performance on flow volume reduction or a validation of model prediction.

For every rainfall event, the volume reduction could be estimated by

1) If $V_{\text{rain}} < V_{\text{storage}}$

Then, $V_{\text{reduction}} = V_{\text{rain}}$, and no overflow

2) If $V_{\text{rain}} > V_{\text{storage}}$

Then, $V_{\text{reduction}} = V_{\text{storage}} + V_{\text{exfiltration}} - V_{\text{infiltration}}$, and overflow appear

The flow chart for this method is shown in Figure 30.

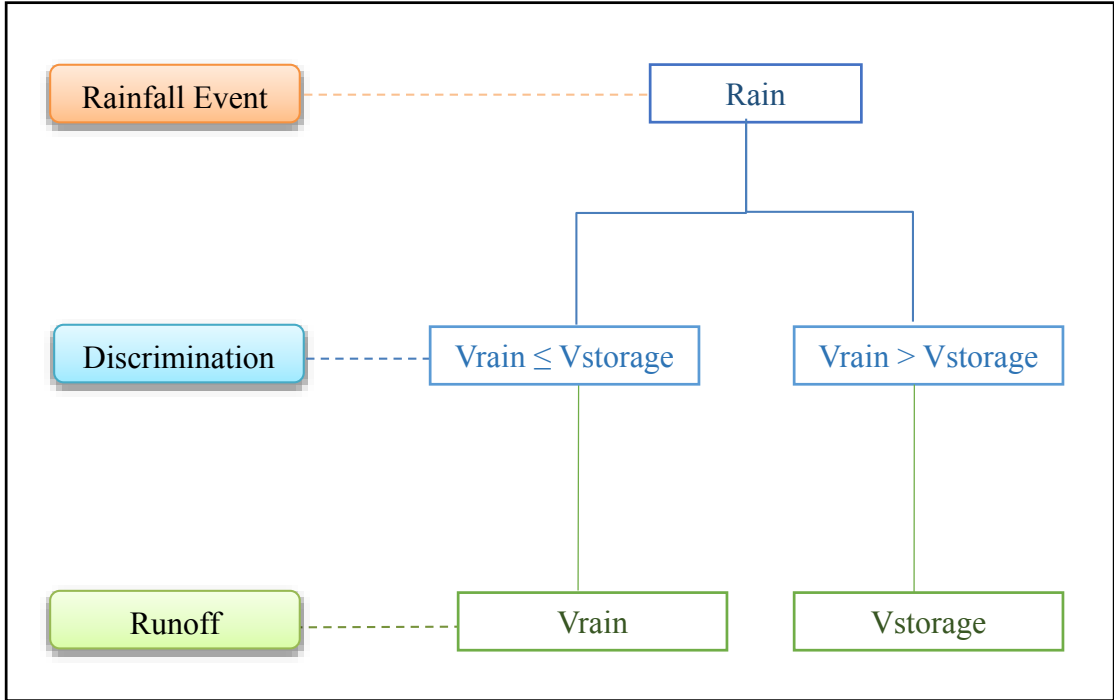


Figure 30. Flow chart for flow volume reduction using stormwater BMPs' design parameters

4.2 Overflow Area Abatement

Coupled 1D/2D hydraulic models are supposed to present a visual contrast in the area of combined sewer overflow before and after the development of the stormwater BMPs. To solve the models in XPSWMM, hydraulic condition/elements and simulation scenarios need to set up according to the practical situation.

4.2.1 Hydraulic Conditions

Elements needed for the coupled 1D/2D models in XPSWMM are composed of 1D elements, 2D elements, and 1D/2D connections. The 1D part simulates the flow conditions in the underground combined sewer system, while the 2D part simulates the overflow on the surface of the ground. Figure 31 is a screenshot of the working station, and all the elements prepared for the coupled 1D/2D hydraulic simulation.

1D Elements

Nodes: represent manholes, catch basin, inlet, wet wells, junctions, ponds or outfalls (Solution). In this study, there are 653 hydraulic nodes in the model, which includes 393 manholes and 260 sewer junctions. The nodes' information on location (Figure 14), spill crest elevation, and invert elevation is necessary for XPSWMM.

Links: represent open channels and river reaches, closed conduits, pumps weirs, orifices and special structures (Solution). In this study, there are 650 hydraulic links (combined sewer pipes) in the model. The links are either single link or multi-link and reflecting location and shape of the buried conduits. There are no gutters, and surface channels located in the study area. The combined sewer pipes were loaded in XPSWMM, together with their upstream nodes, downstream nodes, diameter, slope, length, and roughness. To make sure the accuracy of the pipes' condition, the pipes' length and pipes' slope were updated through XPSWMM's calculating conduit function.

2D Elements

DTM layer: in order to access the topographic data of the study area, the digital terrain model (DTM) is built in the XPSWMM using the topography data in Figure 13. For all the manholes, the elevation of the spill crest of the manholes was adjusted through generating ground elevation from TIN (Triangle Irregular Network) surface.

2D grid layer: an XP2D model grid extents was created both within the range of DTM and the study area. The size of the study area is 292 acres (12718180 ft²). Due to the license of XPSWMM has a 10,000 limit in the number of XP2D cells, the minimum grid step of the XP2D layer has to be 36 ft.

2D inactive layer: in order to prevent stormwater flowing through buildings, the building areas should be either to be set as an inactive layer or given an extremely large Manning's n in the land use layers. In this study the building areas were set as an inactive layer.

Land use layers: the infiltration effect of the ground surface was affected by soil type and land use type. XPSWMM allow users to define the soil type under each land use layer setting. The land use layers in our study include grass layer, trees layer, parking areas layer, road areas layer, driveway areas layer, recreational layer and stormwater BMPs layer. Since the shape file for grass areas is not available, so the grass areas are set as unclaimed areas. Hence, the default land use category was supposed to be set as grass layer. Except for the stormwater BMPs layer, all the other land use layers is active in all the four scenarios.

Head boundary layer: in the default setting, a vertical wall is assumed at the edge of the active grid domain, which will cause water to pile up at the downstream edge of the 2D model. Head boundaries will allow water to exit the flooded area, and three head boundary lines was created on edges of the active area in this study.

2D rain area layer: Rain on the grid method is used in the simulations. Two rainfall/flow area layers were created to coordinate with different scenarios. The status of the rainfall/flow area layer will be discussed in details in the next section.

1D/2D Connections

In the model, it is supposed that the natural dispersal occurs where combined sewer reached its capacity and runoff spreads according to existing topography (Wisheropp, Manha et al.). The manholes' spill crests were linked to the 2D ground surface in the nodes' setting, which can capture inflow from the ground surface.

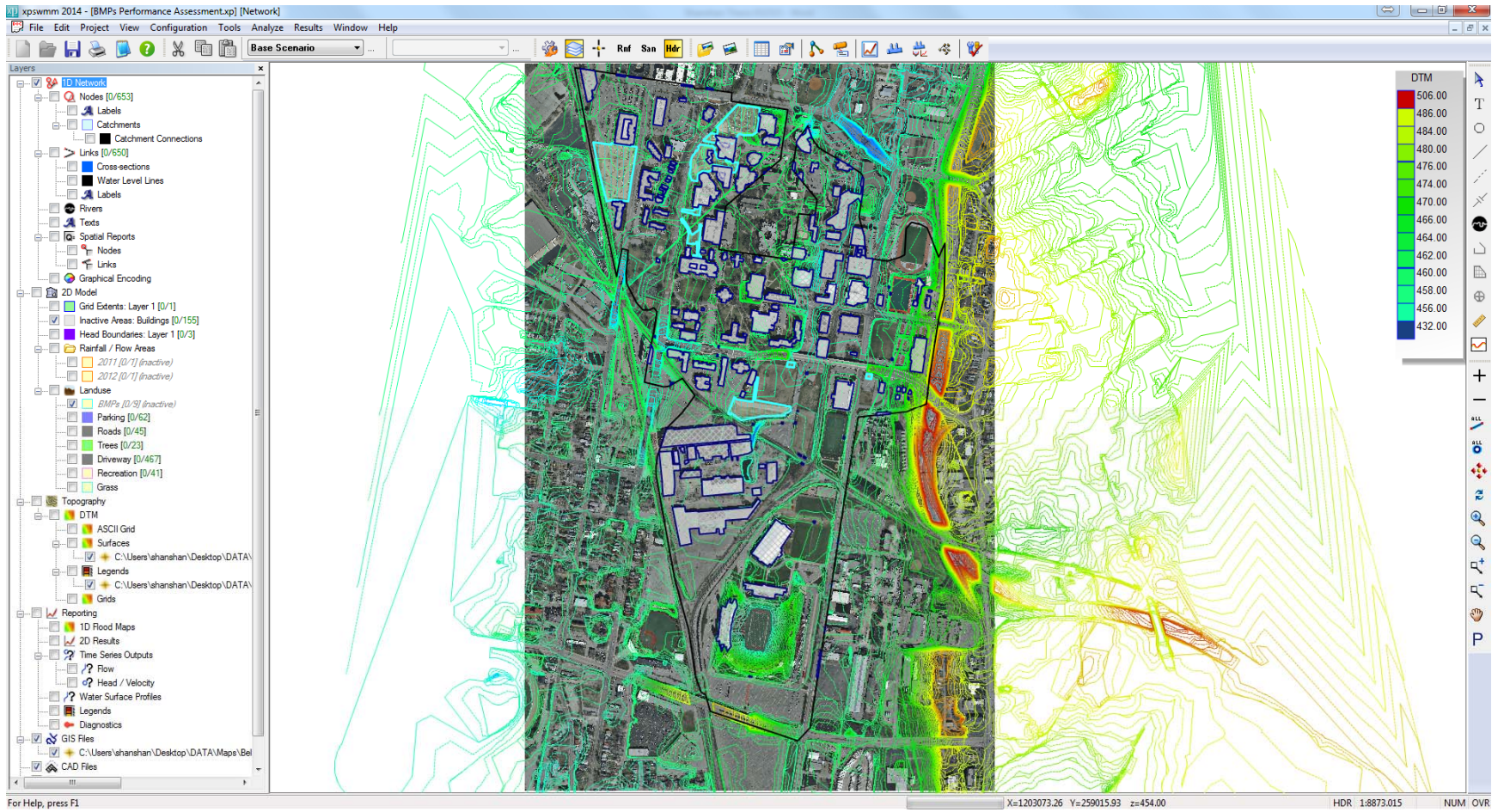


Figure 31 Elements needed in the coupled 1D/2D hydraulic simulation

4.2.2 Simulation Scenarios

In order to obtain the overflow information before and after the development of stormwater BMPs under the two selected rainfall events, four scenarios were studied. The status of the layers under the 1D network, 2D models, and topography for each scenario were listed in Table 15 – 18.

Scenario 1: rainfall event on June 18, 2011

- Scenario 1.1 Overflow Area for Pre-BMPs (Table 15)
- Scenario 1.2 Overflow Area for Post-BMPs (Table 16)

Scenario 2: rainfall event on May 29, 2012

- Scenario 2.1 Overflow Area for Pre-BMPs (Table 17)
- Scenario 2.2 Overflow Area for Post-BMPs (Table 18)

Table 15

Status of the layers for the scenario 1.1

Elements	Category	Layer	Status
1D Network	Sewer System	Nodes	Active
		Links	Active
2D Model	2D Layers	2D Grid	Active
		Inactive Areas	Active
		Head Boundary	Active
	Rainfall Event	June 18, 2011 (1-inch)	Active
		May 29, 2012 (4-inch)	Inactive
	Land Use	Tree Areas	Active
		Parking Areas	Active
Road Areas		Active	
Driveway Areas,		Active	
Recreational Areas		Active	
Stormwater BMPs Area		Inactive	
Topography	Surface	DTM	Active

Table 16

Status of the layers for the scenario 1.2

Elements	Category	Layer	Status
1D Network	Sewer System	Nodes	Active
		Links	Active
2D Model	2D Layers	2D Grid	Active
		Inactive Areas	Active
		Head Boundary	Active
	Rainfall Event	June 18, 2011 (1-inch)	Active
		May 29, 2012 (4-inch)	Inactive
	Land Use	Tree Areas	Active
		Parking Areas	Active
Road Areas		Active	
Driveway Areas,		Active	
Recreational Areas		Active	
Stormwater BMPs Area		Active	
Topography	Surface	DTM	Active

Table 17

Status of the layers for the scenario 2.1

Elements	Category	Layer	Status
1D Network	Sewer System	Nodes	Active
		Links	Active
2D Model	2D Layers	2D Grid	Active
		Inactive Areas	Active
		Head Boundary	Active
	Rainfall Event	June 18, 2011 (1-inch)	Inctive
		May 29, 2012 (4-inch)	Active
	2D Model	Land Use	Tree Areas
Parking Areas			Active
Road Areas			Active
Driveway Areas,			Active
Recreational Areas			Active
Stormwater BMPs Area			Inactive
Topography	Surface	DTM	Active

Table 18

Status of the layers for the scenario 2.2

Elements	Category	Layer	Status
1D Network	Sewer System	Nodes	Active
		Links	Active
2D Model	2D Layers	2D Grid	Active
		Inactive Areas	Active
		Head Boundary	Active
	Rainfall Event	June 18, 2011 (1-inch)	Inactive
		May 29, 2012 (4-inch)	Active
	Land Use	Tree Areas	Active
		Parking Areas	Active
Road Areas		Active	
Driveway Areas,		Active	
Recreational Areas		Active	
Stormwater BMPs Area		Active	
Topography	Surface	DTM	Active

4.2.3 Simulation Job Control

Since this is a coupled 1D/2D hydraulic simulation, hydraulics job control, and 2D job control is needed to be configured in XPSWMM.

Hydraulics Job Control

In this section, the routing control (parameters for routing simulation) and time control (simulation time) need to be set up. Take scenario 1.1 as an example, the simulation time starts at 10:00:00 of June 18th, 2011, and ends at 19:59:59 of that day. The duration of simulation is 10 hours and the simulation time step is set as 5 seconds (Figure 32).

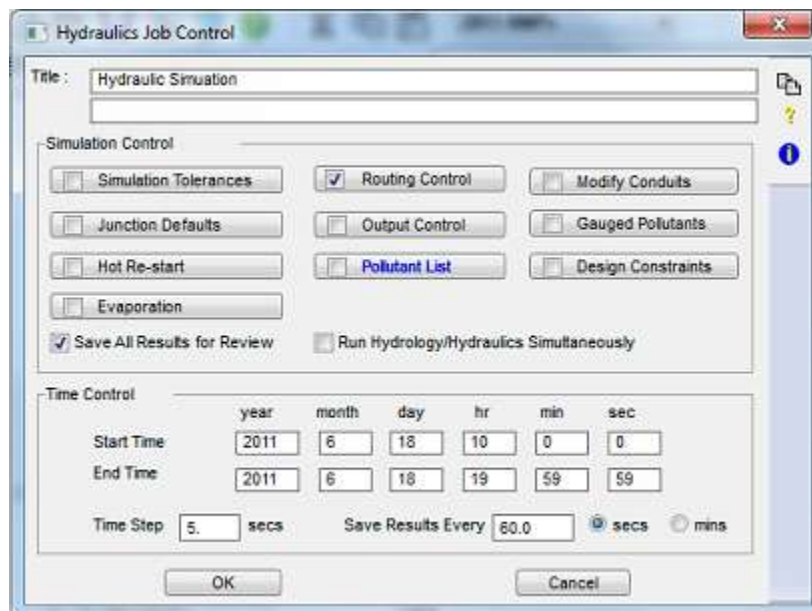


Figure 32 Hydraulics job control interface

2D Job Control

In the 2D job control, the 2D model need to be set active, and the time step is set to 5 seconds. The grass layer is set to be as the default land use category, and the default area type is the active area in this study. Other parameters are using the XPSWMM default values (Figure 33).

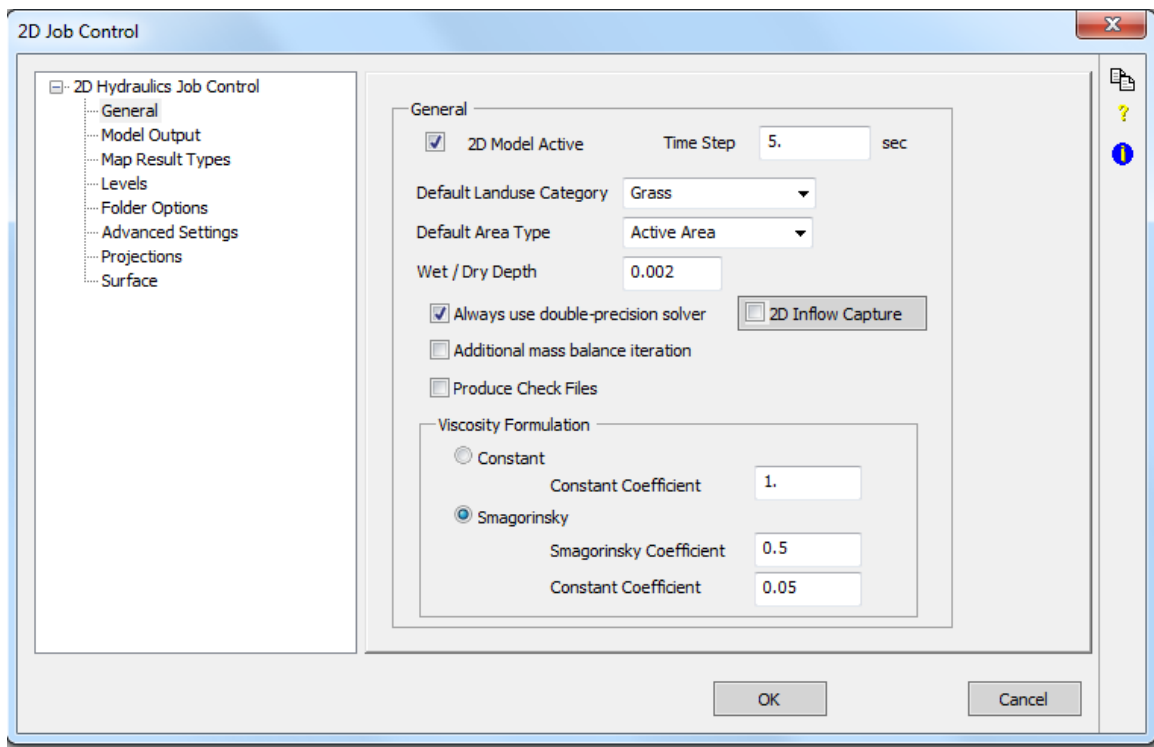


Figure 33 2D job control interface

CHAPTER V

RESULTS AND DISCUSSION

5.1 Flow Volume Reduction

In the previous chapters, the MLRM and BPNNM for flow volume were built by training the rainfall features - flow volume data which is measured before the development of the stormwater BMPs. When the models were applied to predict the flow volume for the rainfall event which occurred after the development of the stormwater BMPs, the predicted/estimated value would be the flow volume generated by the rainfall events without the stormwater BMPs installed in the study area.

It is illustrated in Figure 34 that the predicted flow volume agrees with the trend of actual flow volume of post-development, and almost all of the predicted flow volume are larger than the actual flow volume. It shows that all the estimated flow volume by MLRM is greater than the actual flow volume which was detected by flow meter, and the flow volume reduction ranges from 0.01 to 3.22 million gallons. It is also shown in Figure 34 that of the 109 estimated flow volumes by BPNNM, 102 has an over-estimation, which ranges from 0.04 to 0.88 million gallons.

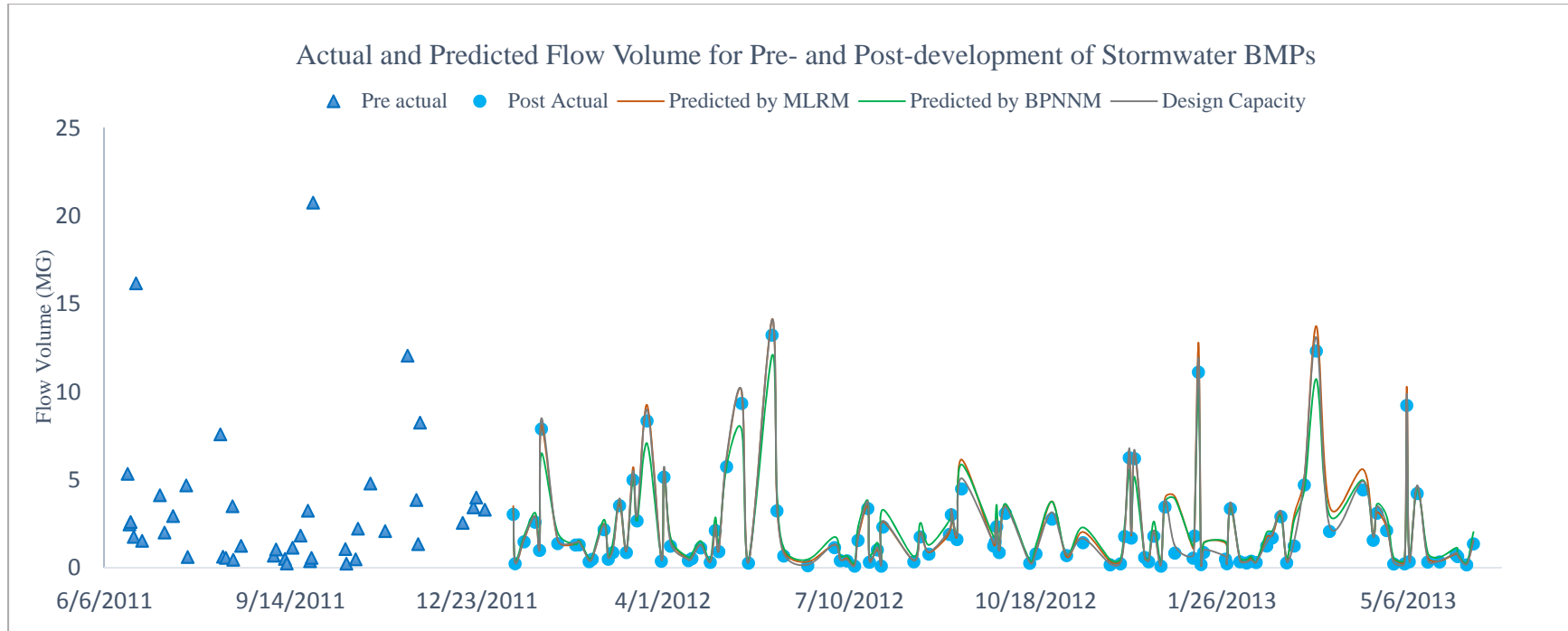


Figure 34 Actual and predicted flow volume for pre- and post-development of stormwater BMPs

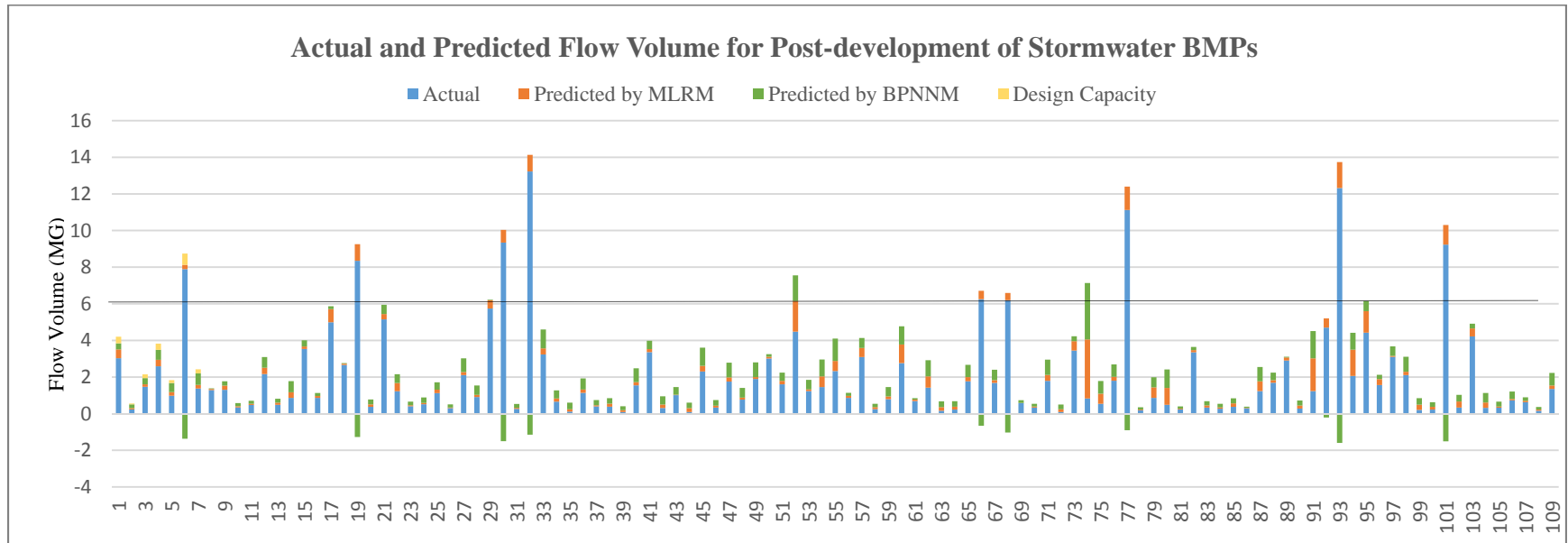


Figure 35 Actual and reduced flow volume for the rainfall events after the development of stormwater BMPs

Seven flow volumes out of the 109 are lower than the actual detected flow volumes. The bar chart in Figure 35 clearly shows: whenever the flow volume is greater than 6 million gallons, the estimation of the flow volume by the BBNNM would be lower than the actual flow volume, which gives a negative value for flow volume reduction. This makes the flow volume BBNNM only applicable to rainfall event which had a flow volume lower than 6 million gallons. There are two possible reasons accountable for this issue:

- (i) The number of total training samples (Pre-BMP rainfall features – flow volume) is relatively small.
- (ii) 85% of training samples having a flow volume less than 6 million gallons.

The predicted/estimated total flow volume reduction for the 109 rainfall events (post-development) by the stormwater BMPs was summarized in Figure 36. It was estimated by flow volume MLRM and BPNNM that the reduction is 38.30 million gallons and 35.12 million gallons respectively. In other words, approximately 14% of the flow was captured/diverted by the stormwater BMPs. The highly identical estimations by the two models also substantiate the feasibility of the multiple linear regression method and back propagation neural network method.

The flow volume reduction can also be estimated by design parameters of the stormwater BMPs. The method was introduced in section 4.1.2.5 Design Parameters. It is estimated that 26.81 million gallons of flow were captured by the stormwater BMPs (Figure 36), which is about 27% lower than the estimations made by flow volume MLRM and BPNNM.

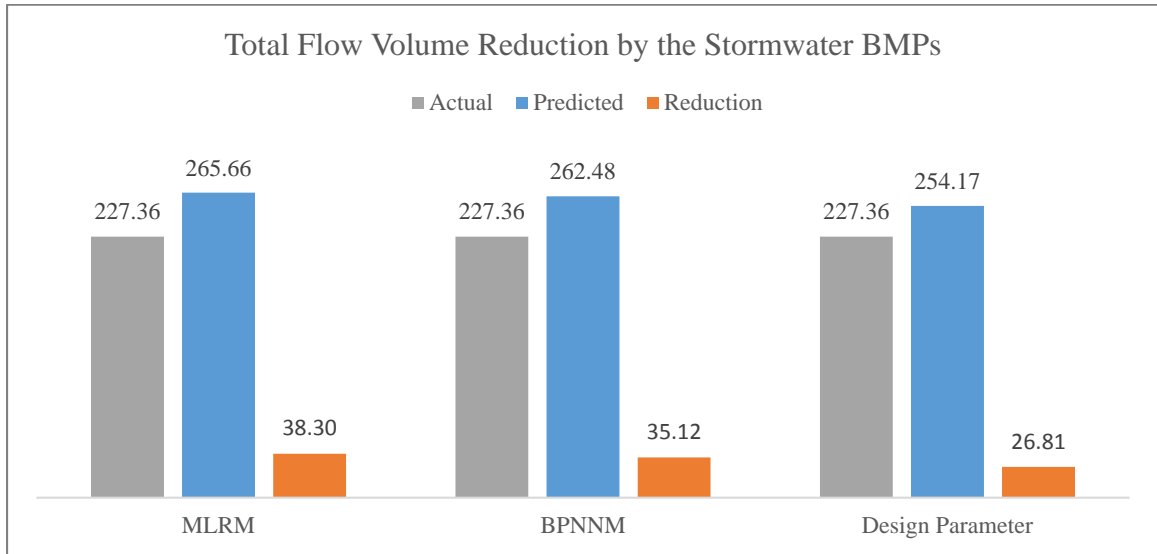


Figure 36 Total flow volume reduction by the stormwater BMPs

5.2 Peak Flow Attenuation

The MLRM and BPNNM for peak flow were also built by training the rainfall features - peak flow on data from before the development of the stormwater BMPs. When the models were applied to predict the peak flow for the rainfall events which occurred after the development of the stormwater BMPs, the predicted/estimated value would be the peak flow generated by the rainfall events without the stormwater BMPs installed in the study area.

It is clearly shown in Figure 37 that the predictions/estimations both from MLRM and BPNNM correlate closely and have a very distinct over-prediction when compared to the actual detected peak flow. Because the models were generated from data obtained prior to installation of the stormwater BMPs, this over-prediction indicates that the stormwater BMPs are having a significant effect on the magnitude of peak flow.

From the results of peak flow MLRM in Figure 37, the magnitude of peak flow in all the 109 rainfall events has been weakened, and the estimated average degree of attenuation is 48.44% (Figure 38). Figure 37 also shows the prediction results from peak flow BPNNM. It illustrates that the magnitude of peak flow in 107 (out of the 109) rainfall events was attenuated, and the estimated average degree of attenuation is 46.28% (Figure 38). The other 2 rainfall events, occurred on April 19, 2013 and March 30, 2013, were estimated to be 1.30 and 2.30 (in million gallons per day) greater than the actual detected peak flow.

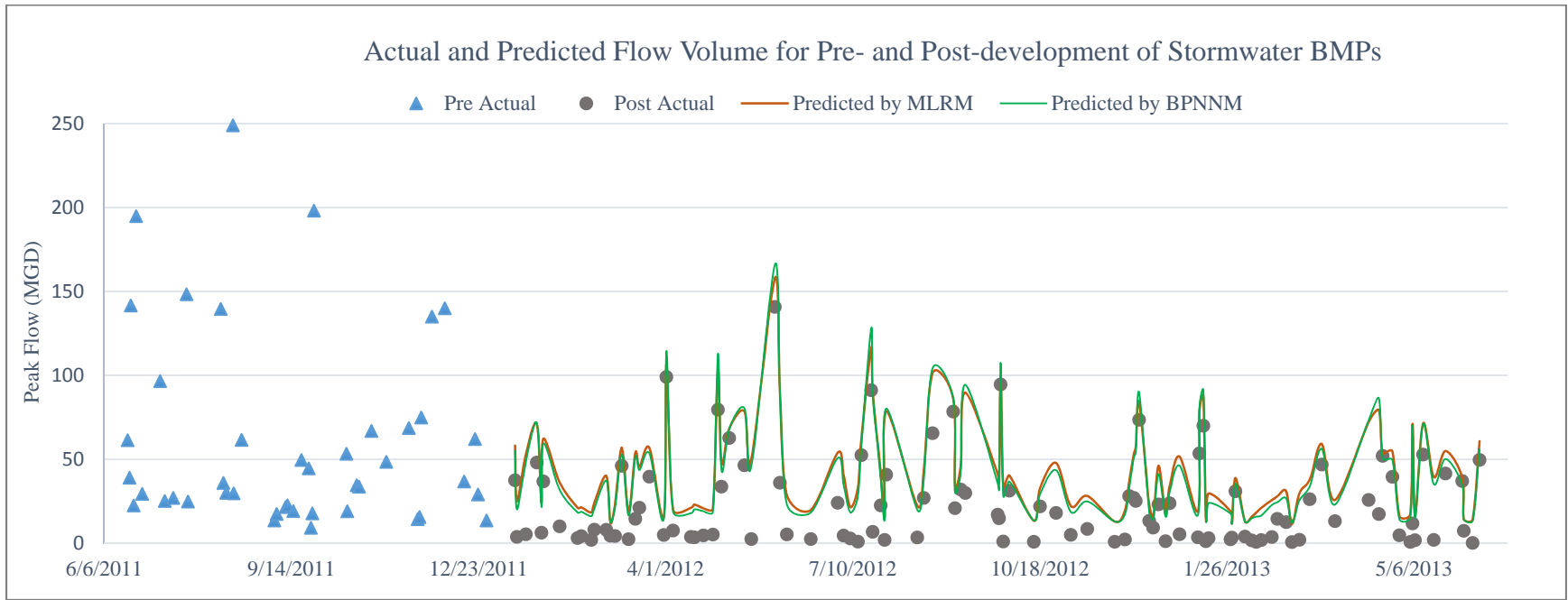


Figure 37 Actual and predicted flow volume for pre- and post-development of stormwater BMPs

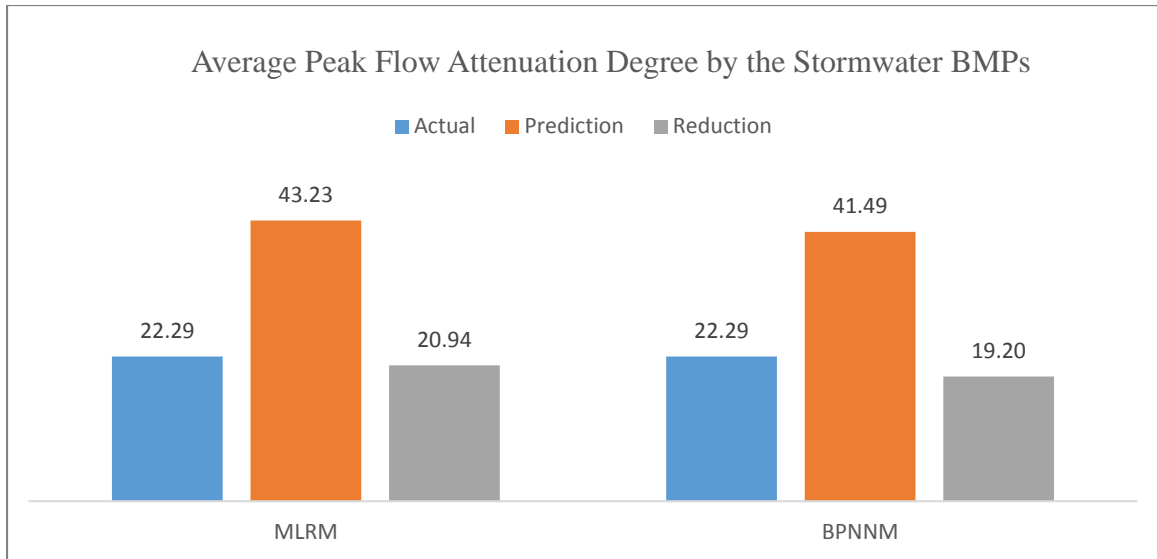


Figure 38 Average peak flow attenuation by stormwater BMPs

5.3 Overflow Area Abatement

The coupled 1D/2D hydraulic models with four scenarios were solved in XPSWMM. The maps of maximum overflow depth for the scenarios were obtained, and the overflow depth animation for each scenario was recorded.

Scenario 1: (1 inch rainfall event on June 18, 2011)

Figure 39 shows the maximum overflow depth for the scenario 1.1 (Pre-BMPs) and scenario 1.2 (Post-BMPs). The blue polygons stand for the areas and locations of the stormwater BMPs. The legend shows the maximum water depth ranges from 0.1 to 6 inches. It shows that almost all of the overflow area has a depth which is below 0.5 inches, except for some areas along Eastern Parkway have a water depth at about 1.5 inches.

There are no significant change on the overflow areas for Pre- and Post BMPs. Therefore, for 1 inch rain, the overflow area is not obviously reduced when the stormwater BMPs is installed. It also reflected the combined sewer's capacity hasn't been reached.

The overflow areas are mostly distributed at the road areas and the concrete areas beside the buildings, but the depth of the overflow is shallow. This is probably because the rain water at this volume tends to pond on the ground surface, instead of flowing into the combined sewer system, or the stormwater BMPs infrastructure.

Scenario 2: (4 inch rainfall event on May 29, 2012)

The 4 inch rainfall occurred on May 29, 2012 generated a larger overflow area than the rainfall occurred on June 18, 2011. Figure 40 shows the maximum overflow depth for the scenario 2.1 (Pre-BMPs) and scenario 2.2 (Post-BMPs) in the study area. The blue polygons stand for the areas and locations of the stormwater BMPs.

It is clear that the majority of the overflow area has a water depth lower than 0.5 inches in both the Pre-BMPs scenario and Post-BMPs scenario. The overflow sensitive areas for the 4 inch rainfall are the areas along the Eastern Parkway, South Brook Street, and South Floyd Street. The depth of overflow in the sensitive area doesn't significantly lowered by the stormwater BMPs. The maximum overflow depth at the T-intersection of Eastern parkway and South 2ND street has reached 6 inches in both the Pre-BMPs scenario and Post-BMPs scenario.

Unlike the 1 inch rainfall event, the 4 inch rainfall event has a distinct contrast on the overflow areas between the Pre-BMPs scenario and Post-BMPs scenario, especially at the location where the stormwater BMPs were installed. It illustrates that the overflow areas at the JB Speed School parking lot, Student Rec Center, and College of Business were significantly abated by the stormwater BMPs.

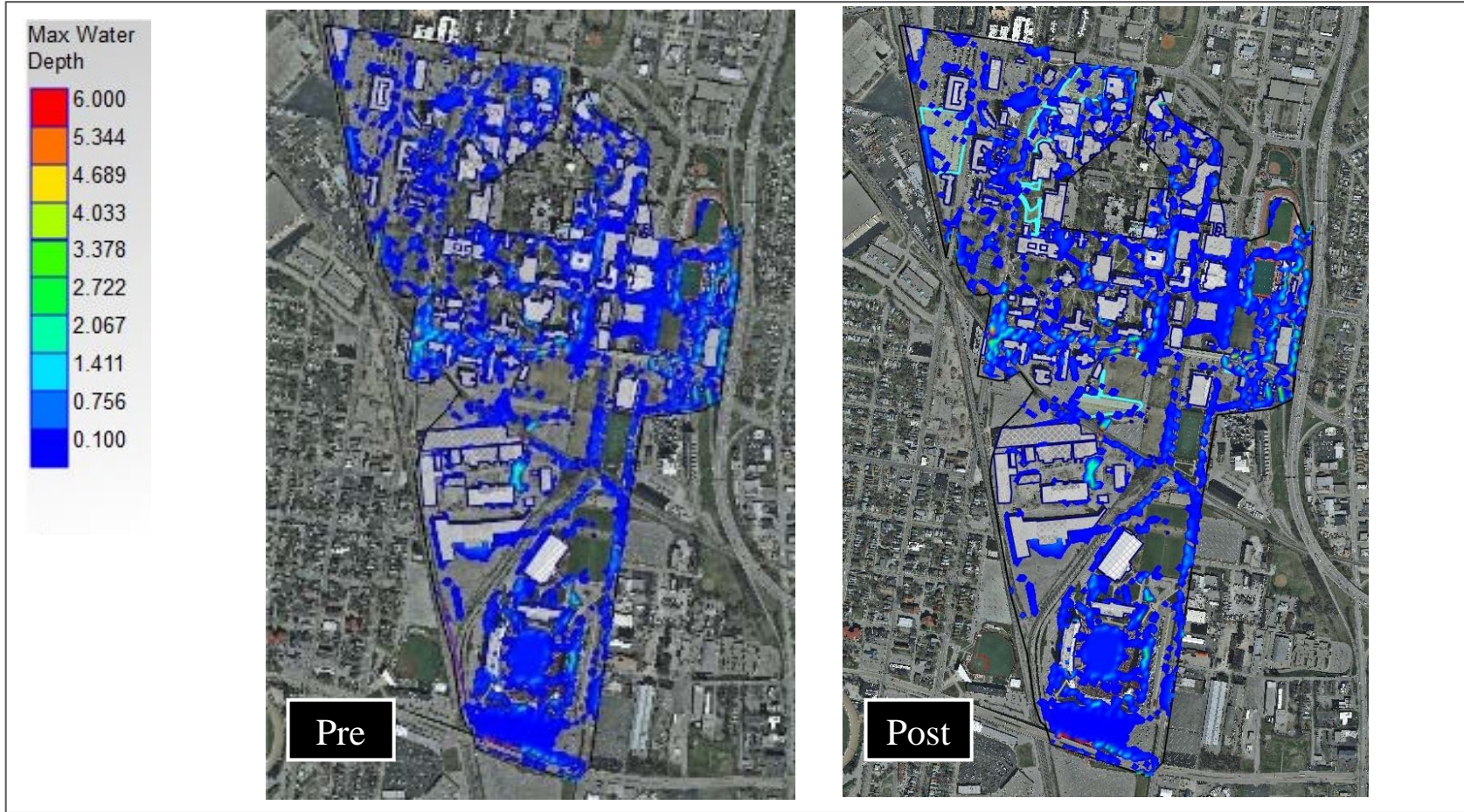


Figure 39 Maximum Pre- and Post-BMPs Overflow Area caused by rainfall event on June 18, 2011

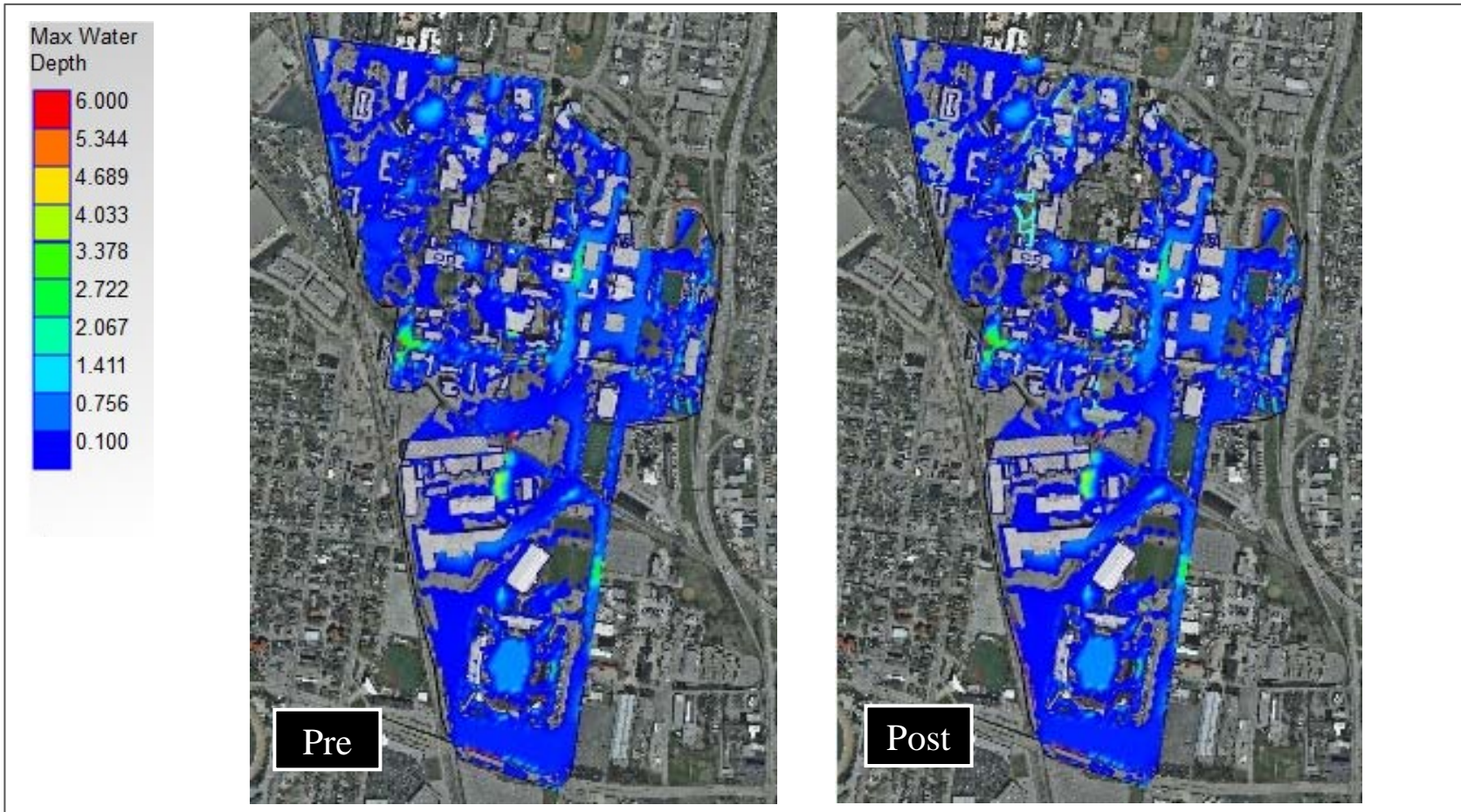


Figure 40 Maximum Pre- and Post-BMPs Overflow Area caused by rainfall event on May 29, 2012

CHAPTER VI

CONCLUSIONS

In this chapter, the conclusions of this research are outlined, and several potential ideas and recommendations for the future work are discussed.

6.1 Conclusions

A comprehensive performance assessment on the stormwater BMPs was accomplished in this study. The assessments were made on three different perspectives: flow volume reduction, peak flow attenuation, and overflow area abatement. The flow volume reduction and the peak flow attenuation were quantified through building Multiple Linear Regression Models (MLRMs) and Back Propagation Neural Network Models (BPNNMs), and the overflow area abatement was visualized by performing coupled 1D/2D hydraulic simulations. The following conclusions are achieved.

(1) The development of stormwater BMPs in the study area have reduced the volume of stormwater flows, attenuated the peak flows, and abated the overflow areas during wet weather.

(2) For the study area, flow volume in wet weather is mostly controlled by rainfall depth, and followed rainfall duration. Peak flow is decided by rainfall depth, peak rainfall intensity, duration and duration of above average rainfall intensity. Peak flow is negatively correlated with rainfall duration, while positively correlated with other three features.

(3) Multiple linear regression and back-propagation neural network are applicable methods in predicting the magnitude of flow volume. However, the flow volume BPNNM is only viable to predict for flow volume lower than 6 million gallons. The estimated volume of the flow diverted by the stormwater BMPs are approximately 30 million gallons per year by both models.

(4) Multiple linear regression and back-propagation neural network are also applicable in predicting the magnitude of peak flow. According to the models' prediction, the magnitude of the peak flow could be trimmed down by approximately 50% after installed the stormwater BMPs.

(5) The coupled 1D/2D hydraulic simulation is a viable tool in visualizing the overflow areas. The overflow areas, which could be saved by the stormwater BMPs, depend on the magnitude of the rainfall event. The abatement in overflow areas is more evident at 4 inch rainfall event and the 1 inch rainfall event. In the 4 inch rainfall event, the overflow areas at the JB Speed School parking lot, Student Rec Center, and College of Business were significantly abated by the stormwater BMPs.

6.2 Contributions

Besides the conclusion of a comprehensive assessment on the stormwater BMPs was reached, here are some additional contributions from this study:

(1) It incorporated peak flow reduction as stormwater BMPs' performance assessment. The of rainfall – runoff assumption raised in this study linked rainfall features with flow volume/peak flow, which brought a new insight in solving stormwater BMPs' assessment problems. The assumption could be revised and adopted in many other situations.

(2) The volume of flow diverted by the stormwater BMPs for every rainfall/storm event in our study period was estimated, and the degree of peak flow attenuated was also predicted by the developed models.

(3) Multiple linear regression and back propagation neural network are feasible method in revealing the relationships either between flow volume and rainfall features, or between peak flow and rainfall features. The prediction accuracy and application range were also discussed.

(4) The overflow course was visualized in a coupled 1D/2D hydraulic simulation, and the overflow sensitive area could provide information needed for stakeholders and decision makers on the stormwater BMPs' installation priority.

6.3 Future Work and Recommendations

The comprehensive performance assessment for the stormwater BMPs was accomplished utilizing the available information. While the assessment methods are applicable in a wide range of cases, the accuracy of the methods still has room to improve. The following are some of the recommendations for the future design and construction of stormwater BMPs.

(1) More flow meters should be installed at the downstream of the combined sewer watersheds, especially for the ones that have severe overflow issues. The predictions on the magnitude of flow volume and peak flow would have been more accurate if more training data were available. Since the study area is comprised of several combined sewer sub-watersheds, flow meters are recommended to be installed at every outlet of the sub-watersheds

(2) If there is more rainfall and flow data available before the development of the stormwater BMPs, antecedent conditions, such as dry period, should be considered as rainfall features in the prediction models. A more accurate model could be obtained through year of rainfall and runoff observation.

(3) Stormwater BMPs need to be installed to alleviate the overflow problem on the T-intersection of Eastern parkway and South 2ND street, because they are the most overflow sensitive areas in wet weather.

(4) More rainfall events should be researched on the overflow areas pre- and post-BMPs installation. For example, 1-year storm, 2-year storm, 5-year storm, 10-year storm, 20-year storm, 50-year storm, and 100-year storm. A reference table could be made for the study area. In this way, once the magnitude of the storm is forecasted or measured, the rough overflow risk could be assessed through quickly looking up the table.

6.4 Limitations

(1) The data mining could be more sophisticated. For example, more information could have been extracted from the training data. Moreover, there are other mining data algorithms could be applied to developing more accurate predictive models.

(2) Some assumptions may be violated. For example, it is assumed that all the rainfall events are independent in this study, however, extreme conditions do exists.

.

REFERENCES

- Battiata, J., K. Collins, D. Hirschman and G. Hoffmann (2010). "The runoff reduction method." Journal of Contemporary Water Research & Education **146**(1): 11-21.
- Blink, S. A., F. Kelly and J. Skupien (2004). NJ Stormwater Best Management Practices Manual, State of New Jersey.
- Chinrungrueng, C. and C. H. Sequin (1995). "Optimal adaptive k-means algorithm with dynamic adjustment of learning rate." Neural Networks, IEEE Transactions on **6**(1): 157-169.
- CleanRiverCampaign. (2014). "Other Green Cities." Retrieved March 23, 2014, from <http://cleanriverscampaign.org/resources/green-cities/>.
- Damodaram, C., M. H. Giacomoni, C. Prakash Khedun, H. Holmes, A. Ryan, W. Saour and E. M. Zechman (2010). Simulation of combined best management practices and low impact development for sustainable stormwater management1, Wiley Online Library.
- De Sousa, M. R. C., F. A. Montalto and S. Spatari (2012). "Using Life Cycle Assessment to Evaluate Green and Grey Combined Sewer Overflow Control Strategies." Journal of Industrial Ecology **16**(6): 901-913.
- ENTRIX, I. (2010). Portland's Green Infrastructure: Quantifying the Health, Energy, and Community Livability Benefits. City of Portland.

EuropeanCommission. (2013). "In-depth Report: The Multifunctionality of Green Infrastructure."from

http://ec.europa.eu/environment/nature/ecosystems/docs/Green_Infrastructure.pdf.

Fox, J. (1991). Regression Diagnostics: An Introduction, SAGE Publications.

GeoSyntec and ASCE (2002). Urban stormwater BMP performance monitoring a guidance manual for meeting the national stormwater BMP database requirements, DIANE Publishing.

Granato, G. E. (2014). "Statistics for stochastic modeling of volume reduction, hydrograph extension, and water-quality treatment by structural stormwater runoff best management practices (BMPs)." U.S. Geological Survey Scientific Investigations Report 2014–5037: 37.

Guyon, I., Andr, #233 and Elisseff (2003). "An introduction to variable and feature selection." J. Mach. Learn. Res. **3**: 1157-1182.

Guyon, I. and A. Elisseff (2003). "An introduction to variable and feature selection." The Journal of Machine Learning Research **3**: 1157-1182.

Hall, M., E. Frank, G. Holmes, B. Pfahringer, P. Reutemann and I. H. witten (2009). "The WEKA Data Mining Software: An Update " SIGKDD Explorations **11**(1).

Hall, M. A. (1999). Correlation-based feature selection for machine learning, The University of Waikato.

Heasom, W., R. G. Traver and A. Welker (2006). "Hydrologic modeling of a bioinfiltration best management practices." JAWRA Journal of the American Water Resources Association **42**(5): 1329-1347.

Hirschman, D., K. Collins and T. Schueler (2008). Virginia Runoff Reduction Method.

Houdeshel, C. D., C. A. Pomeroy, L. Hair and J. Moeller (2010). "Cost-estimating tools for low-impact development best management practices: challenges, limitations, and implications." Journal of Irrigation and Drainage Engineering **137**(3): 183-189.

Hsieh, C.-h. and A. P. Davis (2005). "Evaluation and optimization of bioretention media for treatment of urban storm water runoff." Journal of Environmental Engineering **131**(11): 1521-1531.

Hunt, W., A. Jarrett, J. Smith and L. Sharkey (2006). "Evaluating bioretention hydrology and nutrient removal at three field sites in North Carolina." Journal of Irrigation and Drainage Engineering **132**(6): 600-608.

Infrastructure, T. and G. Infrastructure (2013). "National Stormwater Calculator User's Guide."

Jaffe, M., M. Zellner, E. Minor, M. Gonzalez-Meler, L. B. Cotner, D. Massey, H. Ahmed, M. Elberts, H. Sprague, S. Wise and B. Miller (2010). The Illinois Green Infrastructure Study : a report to the Illinois environmental protection agency on the criteria in section 15 of public act 96-0026, the Illinois green infrastructure for Clean Water Act of 2009.

Kittler, J. (1986). "Feature selection and extraction." Handbook of pattern recognition and image processing: 59-83.

Kohavi, R. (1995). A study of cross-validation and bootstrap for accuracy estimation and model selection. IJCAI.

Krogh, A. and J. Vedelsby (1995). "Neural network ensembles, cross validation, and active learning." Advances in neural information processing systems: 231-238.

- Leandro, J., A. S. Chen, S. Djordjevic and D. A. Savic (2009). "Comparison of 1D/1D and 1D/2D Coupled (Sewer/Surface) Hydraulic Models for Urban Flood Simulation." Journal of Hydraulic Engineering **135**(6): 495-504.
- Li, S., C. Zhang, M. Wang and Y. Li (2014). "Adsorption of multi-heavy metals Zn and Cu onto surficial sediments: modeling and adsorption capacity analysis." Environmental Science and Pollution Research **21**(1): 399-406.
- Liu, L., B. Hoblit, R. Jensen and D. Curtis Automatic gage-adjusted radar rainfall estimation for real-time storm water control.
- Naumann, S., M. Davis, T. Kaphengst, M. Pieterse and M. Rayment (2011). Design, Implementation and Cost Elements of Green Infrastructure projects. Brussels: European Commission.
- Osborne, J. and E. Waters (2002). "Four assumptions of multiple regression that researchers should always test." Practical assessment, research & evaluation **8**(2): 1-9.
- Othman Jaafar, M., E. Toriman, S. S. Mastura, M. B. Gazim, P. I. Lun, P. Abdullah, M. K. A. Kamarudin and N. A. A. Aziz (2010). "Modeling the impacts of ringlet reservoir on downstream hydraulic capacity of Bertam River using XPSWMM in Cameron Highlands, Malaysia." Research Journal of Applied Sciences **5**(2): 47-53.
- Ovbiebo, T. and N. She (1995). Urban runoff quality and quantity modeling in a subbasin of the Duwamish river using XP-SWMM. Watershed Management Planning for the 21st Century, ASCE.
- Passeport, E., W. F. Hunt, D. E. Line, R. A. Smith and R. A. Brown (2009). "Field study of the ability of two grassed bioretention cells to reduce storm-water runoff pollution." Journal of Irrigation and Drainage Engineering **135**(4): 505-510.

Pedersen, L., N. E. Jensen and H. Madsen (2010). "Calibration of Local Area Weather Radar—Identifying significant factors affecting the calibration." Atmospheric Research **97**(1–2): 129-143.

Phillips, B., S. Yu, G. Thompson and N. De Silva (2005). 1D and 2D Modelling of Urban Drainage Systems using XP-SWMM and TUFLOW. 10th International Conference on Urban Drainage, Copenhagen/Denmark.

Reese, A. J. and T. N. Debo (2002). Introduction to Municipal Stormwater Management. Municipal Stormwater Management, Second Edition, CRC Press.

Riedmiller, M. and H. Braun (1993). A direct adaptive method for faster backpropagation learning: The RPROP algorithm. Neural Networks, 1993., IEEE International Conference on, IEEE.

Rossman, L. A. Storm water management model user's manual, version 5.0.

Rushton, B. T. (2001). "Low-impact parking lot design reduces runoff and pollutant loads." Journal of Water Resources Planning and Management **127**(3): 172-179.

Schaefer, R. (2009). The Benefits of CSOnet Based on XPSWMM Model Simulations, Memo to the City of South Bend, IN.

Solution, X. XPSWMM stormwater & wastewater management model getting started manual.

Solutions, X. (2004). Getting Started Manual.

Steiner, M., J. A. Smith, S. J. Burges, C. V. Alonso and R. W. Darden (1999). "Effect of bias adjustment and rain gauge data quality control on radar rainfall estimation." Water Resources Research **35**(8): 2487-2503.

Strassler, E., J. Pritts, K. Strellec and A. Division. (2006, March 06, 2012). "Preliminary Data Summary of Urban Storm Water Best Management Practices." 2014, from <http://water.epa.gov/scitech/wastetech/guide/stormwater/>.

Technology, C. f. N. (2006). "Green Values: National Stormwater Management Calculator." Getting Started Retrieved March 24, 2014, from <http://greenvalues.cnt.org/national/calculator.php>.

Thorndahl, S. and M. R. Rasmussen (2012). "Marine X-band weather radar data calibration." Atmospheric Research **103**(0): 33-44.

Toriman, M. E., A. J. Hassan, M. B. Gazim, M. Mokhtar, S. S. Mastura, O. Jaafar, O. Karim and N. A. A. Aziz (2009). "Integration of 1-D hydrodynamic model and Gis approach in flood management study in Malaysia." Research Journal of Earth Sciences **1**(1): 22-27.

URS (2012). Green Infrastructure Design Manual.

USEPA (2011). Green Long-Term Control Plan-EZ Template: A Planning Tool for Combined Sewer Overflow Control in Small Communities Washington, DC.

USEPA. (2013). "Best Management Practices (BMPs)." Retrieved March 22, 2014, from <http://www.epa.gov/nrmrl/wswrd/wq/stormwater/bmp.html>.

USEPA. (2013, February 1). "Storm Water Management Model (SWMM)." Retrieved 3/22, 2014, from <http://www.epa.gov/nrmrl/wswrd/wq/models/swmm/#Downloads>.

Weiss, P. T., J. S. Gulliver and A. J. Erickson (2007). "Cost and pollutant removal of storm-water treatment practices." Journal of Water Resources Planning and Management **133**(3): 218-229.

Wise, S., J. Braden, D. Ghalayini, J. Grant, C. Kloss, E. MacMullan, S. Morse, F. Montalto, D. Nees, D. Nowak, S. Peck, S. Shaikh and C. Yu (2010). Integrating Valuation Methods to Recognize Green Infrastructure's Multiple Benefits. Low Impact Development 2010: 1123-1143.

Wisheropp, P., A. Manha and C. Entrix Modeling BMP's in Sensitive Areas with xpswmm, King's Beach Watershed Improvement Project.

Yang, Y. and J. O. Pedersen (1997). A Comparative Study on Feature Selection in Text Categorization. Proceedings of the Fourteenth International Conference on Machine Learning, Morgan Kaufmann Publishers Inc.: 412-420.

Zachary Bean, E., W. Frederick Hunt and D. Alan Bidelspach (2007). "Evaluation of four permeable pavement sites in eastern North Carolina for runoff reduction and water quality impacts." Journal of Irrigation and Drainage Engineering **133**(6): 583-592.

APPENDIX

```
import java.io.BufferedWriter;

import java.io.File;

import java.io.FileWriter;

import java.io.IOException;

import java.util.Random;

import weka.classifiers.Evaluation;

import weka.classifiers.functions.MultilayerPerceptron;

import weka.core.Instances;

import weka.core.converters.CSVLoader;

public class Water {

    @SuppressWarnings("resource")

    public static void main(String args[]) throws Exception {

        // File to write the output to.

        BufferedWriter outputWriter = new BufferedWriter(new FileWriter(

            "output.csv"));

        // Get the dataset from file named 'data.csv' or the passed value.

        String fname = "data.csv";

        if (args.length > 0) {

            // This is executed only if there is an input parameter.
```

```

        fname = args[0];
    }

    // Read the dataset from the CSV file.
    Instances dataset = loadTrainingARFF(fname);

    // Set the class index to 'Fp'
    dataset.setClass(dataset.attribute("Fp"));

    // Repeat for different values of l, m, h.
    for (double l = 0.0; l <= 1.0; l = l + 0.1) {
        for (double m = 0.0; m <= 1.0; m = m + 0.1) {
            for (int h = 0; h <= 4; h++) {

                // Build the classifier and set the options.
                MultilayerPerceptron mlp = new MultilayerPerceptron();
                mlp.setLearningRate(l);
                mlp.setMomentum(m);
                mlp.setHiddenLayers(h + "");

                mlp.buildClassifier(dataset);

                // Run the 10-fold cross evaluation.
                Evaluation eval = new Evaluation(dataset);
                eval.crossValidateModel(mlp, dataset, 10, new Random(1));

                // Write the Correlation Coefficient to the output file.
                outputWriter.write(l + "\t" + m + "\t" + h + "\t"

```

```

        + eval.correlationCoefficient() + "\n");
    }
}

// Close the file after writing all the output values.
outputWriter.flush();
outputWriter.close();
// DONE.
System.out.println("Output written to: 'output.csv'");
}

public static Instances loadTrainingARFF(String fname) throws IOException {
    CSVLoader tr = new CSVLoader();
    tr.setSource(new File(fname));
    Instances data = tr.getDataSet();
    return data;
}

```

CURRICULUM VITAE

Shanshan Li

Education

- **2011-2015 PH.D.** Civil and Environmental Engineering, University of Louisville
Thesis: Data driven comprehensive assessment of the performance of stormwater best management practices
- **2008-2011 MEng** Environmental Engineering, North China Electric Power University
Thesis: Studies on the Adsorption Mechanism Models of Heavy Metals and Herbicide onto Main Components in Surficial Sediments
- **2003-2007 BEng** Environmental Engineering, Shandong University of Science and Technology
Thesis: A New Technology on Manufacturing Chemical Materials Using Fly Ash.

Publications

- Ting Wang, **Shanshan Li**, Chen Zhang, Yu Li (2015) Quantities, sources and adsorption of polybrominated diphenyl ethers in components of surficial sediments collected near the sewage draining exits of Jilin City along the Songhua River, China, *Chemosphere*, 119, 1208-1216.
- Xiaoyu Liu, **Shanshan Li**, Yuhang Cai, Long Jiang, Nan Cheng, Wenjin Zhao, Yu Li (2015) Adsorption Mechanism of Estrogens on Soil Studies Based on Density Functional Theory and Quantitative Structure-Activity Relationship Model, *Asian Journal of Chemistry*, 27(4), 1199-1204.
- **Shanshan Li**, Chen Zhang, Meng Wang, Yu Li (2014) Adsorption of multi-heavy metals Zn and Cu onto surficial sediments: modeling and adsorption capacity analysis, *Environmental Science & Pollution Research*, 21(1), 399-426.
- Yu Li, Chen Zhang, **Shanshan Li**, Changzhi Zhou, Xiaoping Li (2014) Single and Competitive Adsorption of 17α -Ethinylestradiol and Bisphenol A with Estrone, β -Estradiol, and Estriol onto Sediment, *Marine Drugs*, 12(3), 1349-1360.
- Yu Li, Meng Wang, Qian Gao, **Shanshan Li** (2012) Establishment of a multiple regression adsorption model for atrazine adsorption onto the surficial sediments with Cu^{2+} present, *Journal of Shenzhen University Science and Engineering*, 29(1), 7-11.
- Qian Gao, Zhizeng Wang, Qian Wang, **Shanshan Li**, Yu Li (2011) Artificial neural network and full factorial design assisted AT-MRAM on Fe oxides, organic materials, and

Fe/Mn oxides in surficial sediments, *Chemical Research in Chinese Universities*, 27(6), 944-948.

- Xianyuan Du, Jianlin Liu, Yang Zhang, **Shanshan Li**, Yan Hu, Li Yu (2011) Relationship between Soil Biototoxicity and Levels of Heavy Metals (Pb, Cd, Cu, Zn, Ni, Cr, Co, Sb, Fe, and Mn) in an Oilfield from China, *Fresenius Environmental Bulletin*, 20(1): 121-126.
- Yu Li, **Shanshan Li**, Qian Gao, Ao Wang (2011) Effect of interaction of non-residual fractions on atrazine adsorption onto surficial sediments and natural surface coating samples, *Chemical Research in Chinese Universities*, 27(2), 212-216.
- **Shanshan Li**, Qian Gao, Xiaoli Wang, Yu Li (2010) Using multiple regression adsorption models to estimate Zn and Cu adsorptions onto Fe oxides, Mn oxides, organic materials and their blends in surficial sediments, *Fresenius Environmental Bulletin*, 19(8): 1466-1473.

Honors and Awards

- Jan 2014 Fellowship Award through January 1st 2014 to April 30th 2015, University of Louisville
- July 2012 Fellowship Award through August 1st 2012 to July 30th 2013, University of Louisville
- Feb 2011 Fellowship Award through August 1st 2011 to July 30th 2012, University of Louisville
- Apr 2011 “Honored Graduate” of North China Electric Power University

- Dec 2010 “Excellent Graduate Student”, North China Electric Power University
- Oct 2006 “Three Good Student”, Shandong University of Science and Technology
- Mar 2006 Excellent CET-4 Performance Award, Shandong University of Science and Technology
- Oct 2005 “Three Good Student”, Shandong University of Science and Technology
- Nov 2004 Knowledge Seeking Award, Shandong University of Science and Technology
- Oct 2004 First prize in English Speaking Contest, Shandong University of Science and Technology

Research Experience

Research Projects

- Influence of the Coexistent Heavy Metals on the Environmental Behavior of Pesticides in River Surficial Sediments, Natural Science Foundation of China (NSFC, 50879025), 2009-2011

My Master's thesis is based on this project, and my responsibility is to study the main interaction effects of components in surficial sediments and biofilms when they absorb heavy metals (Cu, Zn) and herbicide (Atrazine).
- Identification and Classification Technology of Oil Pollution Spectrum in Typical Drilling Area

– A Branch of the State-Supported Project “Ecological Risk Assessment and Key Technology of Pollution Control Studies on Land Oil Drilling” (2008BAC43B01), 2008-2011

I was one of six graduate students (two PhD and four MS students) who were involved in this project. My part was to obtain a raw distribution of heavy metals (Pb, Cd, Cu, Zn, Ni, Cr, Co, Sb, Fe, and Mn) and toxic organic matter (BaP, PHE, ANT, CHR) by performing a statistical analysis of the variation in distance to the oil wells.

Internship experience

- Sept 2006 Studied in the Rizhao waste incinerator plant to learn solid waste treatment technology and percolate treatment technology (UASB).
- Aug 2005 Observed Tuandao, Bohaihe, and Nibuwan Sewage Treatment Plants in Qingdao to learn the theory and operation of the AAO, AB, and Oxidizing ditch technology; visited Gaojiatai Water Supply Company to learn the purification process of running water.
- June 2005 Conducted field research measuring pollutants using HPLC with the local Coal Company.

Conferences

- April 17th, 2014 Attended “Site Supply Workshop” about “Green Infrastructure BMP’s & Earth Stabilization System”, Louisville KY

- Nov 12th-15th 2013 Attended “Five City Plus Conference” about “Integrated Overflow Abatement Plan”, Louisville KY
- Sep 5th, 2012 Attended “Kentucky Water Summit” about “The Kentucky Center of Excellence for Watershed Management”, Lexington KY

Certificate of Achievement

- Green Infrastructure BMP’s & Earth Stabilization System

Skills and Others

- Software: Weka, Minitab, SPSS, ArcGIS, Mat-lab, XPSWMM;
- Measurement Apparatus: HPLC, FAAS
- Being one of the organizers and the Emcee for Chinese Moon Festival Gala in Oct, 2012.

Professional Membership

- American Society of Civil Engineering